Absence of a tough-brittle transition in the statistical fracture of unidirectional composite tapes under local load sharing

S. Mahesh*
Materials Science and Technology Division, Los Alamos National Laboratory, Los Alamos, New Mexico 87544, USA

S. L. Phoenix†
Theoretical and Applied Mechanics, Cornell University, Ithaca, New York 14853, USA

(Received 5 August 2003; published 9 February 2004)

We show analytically that a planar, unidirectional fibrous composite, which is an idealized random heterogeneous material consisting of stiff fibers of random strength embedded in parallel in a compliant matrix, fractures in a brittle manner when the fibers engage in idealized, local load sharing. Both the fibers and matrix are assumed time independent. This brittle behavior occurs irrespective of the disorder (variability) in fiber strengths, which we represent by a power distribution function. Our result goes far toward settling a long-standing question, not resolvable by computer simulations, regarding whether or not the brittle failure regime gives way to a tough, ductile-like failure regime as the variability in fiber strengths is increased past some threshold. We establish this result by calculating upper and lower bounding distributions for composite strength using the Chen-Stein theorem of extreme value statistical theory when failure events are dependent. These bounds both have weakest link character and, by comparing them with empirical strength distributions generated by Monte Carlo simulations, we find that the upper bound is a good approximation to the actual failure probability when the fiber strength variability is large. This regime is where previous models have broken down, raising speculation about a brittle-ductile transition.

DOI: 10.1103/PhysRevE.69.026102 PACS number(s): 62.20.Mk, 05.40.−a

I. INTRODUCTION

In the study of fracture processes and ultimate strength of random heterogeneous materials, the tough-brittle transition is of great importance. This transition, abrupt or otherwise, refers to the qualitative change in the failure mode with microstructural parameter values from one in which material failure occurs by the eventual formation and catastrophic propagation of a single crack (localized damage evolution) to one in which dispersed microscopic cracks form, grow stably, and coalesce to bring about material failure (dispersed damage evolution). The ratio of the volume of damage prior to unstable crack growth to the total volume is small in the former mode, while it is of the order of 1 in the latter mode. The failure mode—brittle or tough—exhibited by the random heterogeneous material determines its strength distribution, and this makes the study of the tough-brittle transition interesting from a technological standpoint as tough behavior is usually preferred.

An example of a random heterogeneous material that fails only by the tough mode is the *loose bundle of fibers* studied by Daniels [1]. It consists of an array of n fibers of equal length whose strengths are randomly distributed, tensioned between rigid horizontal supports [Fig. 1(a)]. Material failure, arising from random fiber breakages, is thus a stochastic process. After breaking, a fiber carries no load; its share of the applied load is assumed to be distributed evenly among the surviving fibers, i.e., the load concentration in each of the $n-r$ surviving fibers after the failure of r fibers is assumed to be

$$K_r^{\mathrm{ELS}}=\frac{n}{n-r}. \tag{1}$$

Such a redistribution of applied load among surviving fibers is called *equal load sharing* (ELS). In such a bundle, the stress concentration on an intact fiber is independent of its physical proximity to a broken fiber and therefore, under increasing applied load, tough failure occurs by dispersed fiber breaking, up to some critical fraction, followed by apparent catastrophic coalescence of the dispersed fiber failures. Daniels [1] established through a highly nontrivial analysis that if n is large and the fiber strengths are indepen-

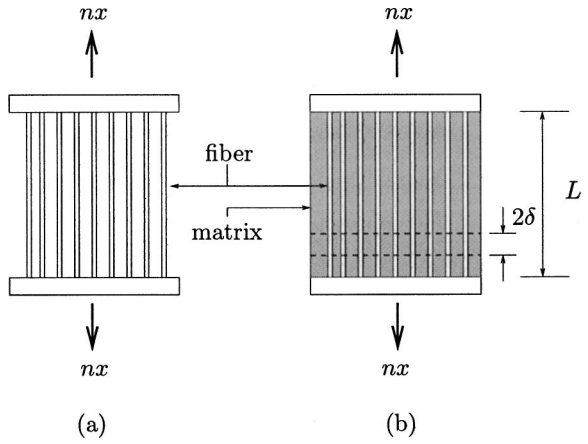

FIG. 1. (a) The loose bundle of fibers of Daniels [1], and (b) a planar composite material with fibers embedded in a matrix.

*Electronic address: mahesh@lanl.gov
†Electronic address: slp6@cornell.edu

dent and identically distributed (i.i.d.) according to the distribution function $F(x)$, such that $\lim_{x\uparrow\infty} x[1-F(x)]=0$, then the strength of a loose bundle of fibers is Gaussian with mean

$$x^*[1-F(x^*)] \tag{2}$$

and standard deviation

$$x^*\sqrt{F(x^*)[1-F(x^*)]}/\sqrt{n}, \tag{3}$$

where x^* is the point where the function $x[1-F(x)]$ has its maximum value (assumed unique). Note that x here denotes the applied load *per fiber*, i.e., the total load applied to the composite is nx. The above statistics refer to x.

More generally, load transfer from broken to intact fibers *will depend* upon their mutual proximity, such as when the stiff fibers of the loose bundle are embedded in a compliant matrix to form a composite [Fig. 1(b)]. If the matrix has a sufficiently large shear modulus, the load dropped by a broken fiber will mostly be communicated to its neighboring intact fibers through matrix shear. In such a composite, we will assume the matrix to always remain intact, and identify composite damage with fiber breakage, and a composite crack with a sequence of neighboring fiber breaks ''near'' each other (to be made precise shortly). Unlike in ELS, a formula giving the composite strength distribution, given an arbitrary fiber strength distribution $F(x)$, has been elusive when load sharing is localized. Special cases of this problem have therefore been pursued over the years by various researchers, with restrictive assumptions on fiber strength statistics and interaction between broken and intact fibers.

Numerous works using either analytical methods or composite failure computer simulations have established that, if the fiber strength variability is small, the composite failure mode will be brittle. They have also gone further to determine the composite strength distribution in this case. Far fewer works, however, have investigated the regime of large fiber strength variability through computer simulations, and it is not at all clear, based on these, whether the brittle mode will continue to be followed as fiber strength variability increases or a tough-brittle transition will occur. The dilemma is basically this: If a sizable crack forms in a composite with large fiber strength variability, it is possible that it will grow catastrophically by sequentially overloading and failing intact fibers surrounding itself, i.e., fail in a brittle manner. On the other hand, it is also possible that considerable dispersed fiber failure precedes the formation of a sufficiently large catastrophic crack, so that composite failure actually occurs as a result of coalescence of dispersed cracks, i.e., failure follows the tough mode. This is seen in computer simulations where composite size is necessarily limited. While the latter possibility is unlikely when the fiber strength variability is small, we cannot rule it out when the fiber strength variability is large, and it will be seen in this work that the failure mode followed depends subtly upon the details of fiber strength statistics determined by fiber flaw character, and load sharing between intact and broken fibers.

To make these qualitative notions precise, we follow Gücer and Gurland [2], Rosen [3], and Scop and Argon [4] in treating the composite as a serial arrangement of mechanically and statistically independent bundles each of length 2δ [Fig. 1(b)]. This so-called chain-of-bundles assumption identifies composite failure as the failure of its weakest bundle. If an n-fiber composite of length L is subjected to tensile load x per fiber and the strength distribution for each of its $m=[L/(2\delta)]$ bundles is $G_n(x)$, then by the chain-of-bundles assumption the composite strength distribution is given by

$$H_{m,n}(x)=1-[1-G_n(x)]^m, \quad x\geqslant 0. \tag{4}$$

The problem of determining the composite strength distribution $H_{m,n}$ is therefore reduced to determining $G_n(x)$, given a load sharing scheme and strength distribution for individual fibers.

Within a bundle in which some fibers are broken, various local load sharing models have been proposed in the literature for how the total applied load nx is distributed among the intact fibers. The simplest model, used in this work, is the idealized local load sharing (LLS) model due to Harlow and Phoenix [5]. In this model, the overload on an intact fiber adjacent to ℓ broken fibers (counting on both sides, except for the first and last fibers in the composite) all along the midplane of a bundle is assumed to be $K_\ell=1+(\ell/2)$. This is equivalent to assuming that each broken fiber transfers half its load to each of its two nearest intact neighbors in the same transverse plane. If the load applied to the composite per fiber is x, an intact fiber adjacent to ℓ broken fibers will carry load $[1+(\ell/2)]x$. A more realistic model for elastic fibers in an elastic matrix is due to Hedgepeth [6]. While Hedgepeth's model assigns stress concentrations to the fibers adjacent to a cluster of breaks, some of the load is distributed to fibers further away, the amounts decreasing quickly with distance. However, his model is too complicated for the probability methods of the present work.

The Weibull distribution [7] is often used to model the random strength X of fibers. For a fiber segment of length 2δ,

$$F(x)=\mathrm{Prob}\{X\leqslant x\}=1-\exp[-(2\delta/L_0)(x/x_0)^\rho], \quad x\geqslant 0. \tag{5}$$

Here ρ is called the shape parameter and x_0 is the scale parameter relative to length L_0, the gauge length in tension testing. The study of bundle failure is simplified by assuming that a break anywhere in a 2δ long fiber segment can be repositioned to its center. Also, if $x\ll x_0$ (i.e., in the lower tail), the Weibull distribution is well approximated by the power law distribution

$$F(x)\approx\frac{2\delta}{L_0}\left(\frac{x}{x_0}\right)^\rho. \tag{6}$$

In what follows, we take $(2\delta/L_0)(1/x_0^\rho)=1$ with no loss in generality; an alternative view-point is that x denotes the x of Eq. (6) normalized by $[L_0/(2\delta)]^{(1/\rho)}x_0$, and thus $F(x)=x^\rho$. In view of these assumptions about the load sharing and fiber strength within each bundle, the question posed earlier can be reworded as follows: In a planar composite bundle obeying LLS, is there a tough-brittle transition as ρ decreases, i.e., as the variance in fiber strength increases?

The brittle and tough failure modes, qualitatively described above as composite failure by catastrophic crack extension or coalescence of a number of smaller cracks, respectively, were characterized by Harlow and Phoenix [5] in terms of the bundle strength distribution. By enumerating all possible sequences of fiber breakage leading up to bundle failure, and adding up their probabilities to find $G_n(x)$ for $n=1,2,\ldots,9$, they numerically found that there exists a characteristic distribution function $W(x)$ independent of n for $\rho=5$, 10, and 15 such that

$$W_n(x)\equiv 1-[1-G_n(x)]^{1/n} \xrightarrow{n\uparrow\infty} W(x) \quad \text{for} \quad x>0. \quad (7)$$

They found that convergence is rapid: at $x=0.35$ for $\rho=10$, $|W_n(x)-W_{n+1}(x)|<10^{-11}$ for $n\geqslant 5$, and that the speed of convergence increases with ρ. They also found that such a characteristic distribution function does not exist for a loose bundle of fibers, which fails in a tough manner. Thus, they characterized the brittle failure mode as one in which the composite strength distribution admits a weakest link scaling, Eq. (7). Conversely, in the tough failure mode, they showed that this scaling does not hold. Harlow and Phoenix's conclusions have since been verified on much larger composites (a few thousand fibers) than $n=9$ using efficient recursion algorithms due to Zhang and Ding [8] and Wu and Leath [9].

Harlow and Phoenix [5] reason that $W(x)$ represents the probability of failure of one of n weak links in the bundle. Harlow and Phoenix [10] and Smith [11] identify the physical event corresponding to the failure of a weak link: the formation of clusters of breaks starting from a single ''seed'' fiber break (with probability x^ρ), and its growth by failing at least one of its two neighbors (with probability $1-[1-(K_jx)^\rho]^2$, $j=1,2,\ldots,\kappa-1$, which for small $(K_jx)^\rho$ is approximately $2(K_jx)^\rho$). In the limit as $n\to\infty$ and $\rho\to\infty$ with $\log n/\rho\to c, 0<c<\infty$, Smith proves that $G_n(x)$ will converge to

$$\begin{aligned} G_n(x) &\approx nx^\rho[2(K_1x)^\rho][2(K_2x)^\rho]\cdots[2(K_{\kappa-1}x)^\rho] \\ &= n2^{\kappa-1}K_1^\rho K_2^\rho\cdots K_{\kappa-1}^\rho x^{\kappa\rho}, \end{aligned} \quad (8)$$

where $K_\ell=1+\ell/2$ and κ is the so-called *critical cluster size* and is the integer that satisfies $K_{\kappa-1}x<1<K_\kappa x$. Remarkably, when compared with empirical distributions from Monte Carlo simulations, it is found that Smith's formula is accurate for ρ as small as 3. A possible reason why Smith's formula breaks down for smaller ρ is seen by examining the factor $2(K_jx)^\rho$ in Eq. (8). His model assumes that each of the two fibers surrounding the j cluster is ''fresh,'' i.e., that neither of them has survived a previous overload. The failure probability of a fiber at load $(K_jx)^\rho$ conditional on the event that it has survived load $K_{j-1}x$ is

$$\frac{(K_jx)^\rho-(K_{j-1}x)^\rho}{1-(K_{j-1}x)^\rho}, \quad (9)$$

which, while close to $(K_jx)^\rho$ for large ρ, is much smaller for small ρ. In this respect, Smith's formula overestimates the probability of cluster extension. Note that replacing each factor $(K_jx)^\rho$ in Eq. (8) by Eq. (9) does not improve the agreement. In fact, this correction is excessive and the resulting formula greatly underestimates the failure probability.

The conclusion of Harlow and Phoenix [5] about the existence of a characteristic distribution function $W(x)$ was proved rigorously by Kuo and Phoenix [12] using a renewal theory argument for $\rho\geqslant 3$. They also suggested a way to tighten their argument for $\rho>2$. This did not guarantee, however, that the probability of failure of a large bundle was truly represented by a weakest-link arrangement of n links each following $W(x)$, the stumbling block being the relative magnitude of error resulting from nondominating eigenvalues compared to the dominating one $1-W(x)$.

To get a sense of the form of the distribution for composite strength for a wide range of possible fiber strength statistics, Harlow [13] further simplified the bundle model above and considered a LLS bundle in which fiber strengths are either 0 or 1 with probabilities p and $1-p$, respectively. He set up a primitive recursion matrix which gives the probability of failure of a $(j+1)$-fiber bundle given the probability of failure of a j-fiber bundle and using the Perron-Frobenius theorem proved the existence of the characteristic distribution function in this case, and the true weakest-link probability structure in the lower tail (relevant to large bundles) for arbitrary p. Duxbury and Leath [14] also conducted a similar recursive, eigenvalue based analysis but obtained a simpler analytical result for the lower tail of $W(x)$. Harlow and Phoenix [15] treated the same problem using the Chen-Stein method for the Poisson approximation and obtained an expression for the composite strength distribution for large bundles equivalent to that of Duxbury and Leath [14]. The advantage of the Chen-Stein approach, used in the present work, over the Perron-Frobenius approach is that it gives a closed form expression for both failure probability and a bound on the error resulting from nondominating eigenvalues of the recursion matrix.

Phoenix and Beyerlein [16] consider the 0-1 fiber model as above, but imposed a more dispersed version of LLS, called tapered load sharing, in which the load of a failed fiber is distributed to the nearest and next nearest neighbors in a 2:1 ratio. In this case too, they found explicit asymptotic expressions for $W(x)$, especially in the lower tail, and showed rigorously that a composite under 0-1 fiber strength admits a weakest link scaling in terms of $W(x)$, with diminishing relative error as the bundle size n increases, i.e., undergoes brittle failure, regardless of the probability p that a fiber has 0 strength.

Recently, the statistics of the failure process and ultimate strength in composites have been studied extensively using Monte Carlo computer simulations (e.g., Beyerlein and Phoenix [17], Landis *et al.* [18], and Wu and Leath [19]). These studies go beyond the simplest planar LLS composite bundles and are able to model failure of two- (2D) and three-dimensional (3D) composites incorporating more complicated but realistic load sharing schemes based on a true micromechanical analysis. Load concentration still occurs on fibers next to clusters of broken fibers, but the load eventually grows as the square root of cluster size, with more dis-

tant fibers taking up the remainder. These simulations are limited, however, to modest bundle or composite sizes due to rapidly increasing failure sequence sizes and pattern complexity, and in the case of large variance in fiber strength this can lead to egregious uncertainties in the results, as revealed by the following example.

Assuming Hedgepeth and Van Dyke [20] load sharing, and Weibull fibers in a 3D bundle with hexagonally arrayed fibers, Mahesh *et al.* [[21], Fig. 13] find that a weakest-link scaling, Eq. (7), exists down to $\rho=1$ for bundles with more than 225 fibers and that the characteristic distribution function $W(x)$ can be captured reasonably well with a Smith-like model based on Eq. (8). Using the same empirical distribution data, however, they also obtain agreement with the two-scale model of fracture due to Curtin [22,23]. In his view the composite fails in a brittle matter with the failure of any subsystem (group of a certain number of fibers), but the failure of the subsystem itself falls in the tough failure regime [[21], Fig. 18]. To determine which of these possibilities is true as composite size increases (and only one, if either, can be true), would require knowledge of the lower tail of the bundle strength distribution. Such is not presently obtainable due to computational and algorithmic limitations. Analytical results are therefore essential in putting approximate analyses and interpretations from Monte Carlo simulations on firmer ground.

We must mention here the extensive work on the closely related problem of composite lifetime in which fibers have random lifetimes depending on their load histories (Curtin and Scher [24–26], Newman and Phoenix [27]). A brittle-tough transition does occur in this case at $\rho=1$. Also, owing to their similarity to mechanical fracture, we mention studies of conduction breakdown in random fuse networks and element breakdown in elastic spring networks. A review of these works and their relationship to the present model of composite fracture can be found in Phoenix and Beyerlein [16].

In this work we develop bounds on $G_n(x)$ for a planar, n-fiber LLS bundle for all ρ both from above and below. Our approach will be as follows: We first consider a composite whose fibers can take on one of $r \ll n$ distinct strength values following a prescribed *discrete distribution*. Section II A describes this composite. Sections II B–II E are devoted to estimating the strength distribution of such a composite together with error bounds on the estimate using induction, and the Chen-Stein theorem of extreme value statistics. With this result for the discrete strength case in hand, we then proceed to bound the strength of a composite whose fibers are distributed according to a continuous power law, which guides the choice of discrete probabilities and associated strength values. These bounds are obtained in Sec. III by sandwiching the continuous power law distribution between two discrete strength distributions and applying the result of Sec. II E. The main results are in Sec. IV, where we compare the present bounds with predicted forms of the bundle strength distribution of previous heuristic models in the literature, thought to be valid (based on comparison with Monte Carlo generated strength distributions) for $\rho>1$ but not for smaller ρ. We will show that these heuristic distributions are slightly incorrect even for large ρ and point out why this may not be apparent within the probabilistic range of the simulations. By arriving at the correct scaling of the number of fibers susceptible to failure ahead of a cluster of breaks in Eq. (90), we will also show how these heuristic formulas can be amended to make them applicable to all $\rho>0$.

II. BUNDLES WITH DISCRETE FIBER STRENGTH

A. Notation

Let $I=\{1,2,\ldots,n\}$ be an index set used to number the fibers in a bundle and let $(Z_i : i \in I)$ be i.i.d. random variables distributed according to $\text{Prob}\{Z_i=0\}=\beta_0 \equiv \alpha, \text{Prob}\{Z_i=1\}=\beta_1, \text{Prob}\{Z_i=2\}=\beta_2, \ldots, \text{Prob}\{Z_i=r\}=\beta_r$ where $\alpha+\beta_1+\beta_2+\cdots+\beta_r=1$, and $\beta_j>0$ for $j=0,1,\ldots,r$, which will be used in constructing discrete fiber strengths. Since we repeatedly discuss the event $\cup_{j=q}^{p}\{Z_i=j\}$, where p and q are integers with $0\leqslant q<p\leqslant r$, in what follows, it will be helpful to introduce a shorthand notation for it. We will henceforth take $\{Z_i \in p_q\}$ to be synonymous with $\{Z_i \in \{q, q+1, \ldots, p\}\}$. Then $\text{Prob}\{Z_i=p_q\}=\Sigma_{j=q}^{p}\beta_j$. For example, if we specify $\{Z_i=3_1\}$, it implies the event $\{Z_i=1\}\cup\{Z_i=2\}\cup\{Z_i=3\}$. Also, let us define

$$\gamma_j \equiv \frac{\alpha}{\alpha+\beta_1+\cdots+\beta_j} \tag{10}$$

for $j=1,2,\ldots,r$ and $\gamma_0 \equiv 1$.

Consider an n-fiber LLS bundle whose n fibers are indexed by the set I. Let the strength S_i of its ith fiber be σ_{Z_i} where $0\leqslant\sigma_0<\sigma_1<\sigma_2<\cdots<\sigma_r$ are arbitrary but fixed real numbers. Let this bundle be subjected to a far-field tensile load nx in the fiber direction (we take the fiber cross-sectional area as unity) so that the normalized stress per fiber is x. If $x<\sigma_0$ or $\sigma_r\leqslant x$, all the fibers and hence the bundle, survive or fail, respectively, with probability 1. If, however, $\sigma_0\leqslant x<\sigma_r$, the applied stress x initially causes partial failure of the bundle by breaking those fibers whose strengths are smaller than x. We assume that failure of individual fibers overloads their neighbors according to the idealized local load sharing model described in Sec. I. Some of the overloaded fibers may fail and produce even greater overloads on the remaining intact fibers. This process of fiber breaking followed by intact fiber overloading may eventually lead to failure of all the fibers in the bundle, i.e., catastrophic bundle failure. We wish to calculate the probability of this event.

Next we define non-negative integers $(\ell_j \in \mathbb{Z}_+ : j=0,1,\ldots,r)$ such that $[1+(\ell_j-1)/2]x<\sigma_j\leqslant[1+(\ell_j/2)]x$ if $\sigma_j\geqslant x$ and $\ell_j=0$ if $\sigma_j<x$. That is, ℓ_j is the smallest number of broken neighbors that must surround an intact fiber of strength σ_j in order to overload it to failure under applied load x. We may assume $\ell_0<\ell_1<\ell_2<\cdots<\ell_r$ for, if $\ell_j=\ell_{j+1}$ for some $j\in\{0,1,2,\ldots,r-1\}$, then fibers of strength σ_j and σ_{j+1} are indistinguishable in terms of their failure behavior at fixed applied x and we may eliminate one, say ℓ_{j+1}, from consideration and set $\text{Prob}\{Z_i=j\}=\beta_j+\beta_{j+1}$.

Let X_n denote the smallest applied tensile stress x at which the bundle fails; X_n is then called the bundle strength.

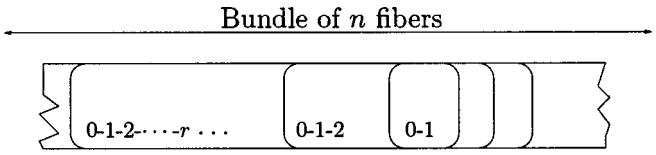

FIG. 2. The dominant failure event in a 0-1-2-$\cdots$-r sub-bundle schematically showing the successively nested failing sub-bundles 0-1, 0-1-2, . . . , 0-1-2-$\cdots$-$(r-1)$. The view shown is a part of the cross section of an n-fiber bundle.

We seek its distribution function $G_n(x)=\text{Prob}\{X_n\leqslant x\}$ for $x\geqslant 0$. The analysis is readily extended to a chain of m statistically independent such bundles each consisting of n fibers. Letting the strength of the chain be that of its weakest bundle, and denoted as $X_{m,n}$, its distribution function is readily obtained once $G_n(x)$ is known, and is $H_{m,n}(x)=\text{Prob}\{X_{m,n}\leqslant x\}=1-[1-G_n(x)]^m$ for $x\geqslant 0$ due to the serial nature of the assemblage.

For the purpose of an overview of the analysis to follow in subsequent sections, we give here a short sketch of the arguments made. In what follows, a *sub-bundle* will refer to some collection of contiguous fibers of the n-fiber bundle. We begin in Sec. II B by evaluating the probability of failure of a sub-bundle within which its fibers are restricted to have strengths σ_0 and σ_1 (to be called a 0-1 sub-bundle). The approach follows that of Harlow and Phoenix [15] although we pay more attention here to the effects of the two sub-bundle boundaries. Then in Sec. II C we consider all the possible ways in which a sub-bundle whose fibers are allowed strengths σ_0, σ_1, and σ_2 (denoted a 0-1-2 sub-bundle) can fail. By evaluating the probability of each of these *failure configurations* we show that two of the configurations asymptotically dominate the rest in the magnitudes of their probabilities of occurrence. These two dominant 0-1-2 configurations contain a 0-1 sub-bundle in them; to evaluate the failure probability of the 0-1-2 sub-bundle one therefore needs the probability of failure of a 0-1 sub-bundle evaluated in Sec. II B. Continuing this process inductively to a 0-1-2-3 sub-bundle, we have in that case another set of failure configurations, all but two of whose probabilities turn out to be asymptotically negligible. These two failure configurations similarly involve a 0-1-2 sub-bundle. As depicted schematically in Fig. 2 we will find that the two asymptotically dominant failure events of a 0-1-2-$\cdots$-r sub-bundle consist of successively nested failing sub-bundles of lower order. Their probabilities of occurrence, $\mu_r(n)$ as given in Eq. (55), constitute our first main result for the strength distribution of a 0-1-2-$\cdots$-r bundle. The error bounds on $\mu_r(n)$ become smaller asymptotically as $\ell_1\wedge(\ell_2-\ell_1)\wedge\cdots\wedge(\ell_r-\ell_{r-1})\wedge(n-\ell_r)\to\infty$.

B. Strength of a 0-1 sub-bundle

Let $I_1=\{p,p+1,\ldots,p+n_1-1\}\subset I, p\leqslant n-n_1+1$, be the index set of an n_1-fiber sub-bundle starting at fiber p in the n-fiber bundle such that $Z_i=1_0$ for $i\in I_1$, i.e., all the fibers within the sub-bundle indexed by I_1 have strength either σ_0 or σ_1. Let $Z_i, i\in I_1$, be distributed as stated in Sec. II A so that the probability of occurrence of a sub-bundle consisting entirely of fibers with $Z_i=1_0$ is $(\alpha+\beta_1)^{n_1}$ for any p. Let $n_1\geqslant\ell_1$. We also define two imaginary fibers at positions $p-1$ and $p-2$ such that $Z_{p-1}=Z_{p-2}=1$. Observe that the sub-bundle indexed by I_1 fails if and only if the sub-bundle indexed by $I_1\cup\{p-2,p-1\}$ fails, so that their probabilities of occurrence are equal. As will be seen shortly, these imaginary left boundary fibers simplify the consideration of failure configurations close to the boundary while leaving the probability of failure of the sub-bundle unchanged.

We now approximate the probability of failure of this sub-bundle, called a 0-1 sub-bundle, using the Chen-Stein method. We begin by defining events associated with fiber $i\in I_1\cup\{p-2,p-1\}$ that produce $Y_i=1$ where Y_i is the dependent Bernoulli process defined in Appendix A. Following Harlow and Phoenix [15] we define the event $Y_i=1, i\in I_1$, if $Z_i=1, Z_{i+\ell_1+1}=0, i+\ell_1+1\in I_1$, and there is exactly one 1 among $Z_{i+1}, Z_{i+2}, \ldots, Z_{i+\ell_1}$. Otherwise we set $Y_i=0$.

It is convenient to express this definition pictorially as

$$\begin{array}{l} i \qquad\qquad\qquad\quad \downarrow \\ 1\underbrace{0\ \cdots\ 0}_{0\leq s<\ell_1}1\underbrace{0\ \cdots\ 0}_{\ell_1-s} \end{array} \tag{11}$$

and henceforth we refer to such depicted occurrences of $Y_i=1$ as failure configurations in the sub-bundle indexed by I_1 since if they occur the sub-bundle fails. Observe that we have not shown the $n_1-(\ell_1+2)$ 1_0 fibers surrounding this configuration in the sub-bundle. On this configuration, we have marked fiber i and have also labeled the *pressured* element with a $\downarrow$. This pressured fiber is surrounded by at least ℓ_1 broken fibers so that it will fail. Note that the failure of the pressured fiber results in catastrophic failure of the 0-1 sub-bundle since it implies that all other 1's in it will be overloaded as well.

Following the Chen-Stein method (see Appendix A), we first evaluate $\text{Prob}\{Y_i=1\}$ as

$$\mathbf{E}[Y_i]\equiv\text{Prob}\{Y_i=1\}=\begin{cases}\alpha^{\ell_1}(\alpha+\beta_1)^{n_1-\ell_1}, & \text{if } i=p-2,\\ \ell_1\beta_1\alpha^{\ell_1}(\alpha+\beta_1)^{n_1-(\ell_1+1)}, & \text{if } i=p-1,\\ \ell_1\beta_1^2\alpha^{\ell_1}(\alpha+\beta_1)^{n_1-(\ell_1+2)}, & \text{if } p\leqslant i<p+n_1-\ell_1-1,\\ 0, & \text{if } i\geqslant p+n_1-\ell_1-1,\end{cases} \tag{12}$$

where $Y_{p-2}=1$ if the event

$$\begin{array}{cccc} p-2 & p-1 & & \\ & \downarrow & & \\ 1 & 1 & \underbrace{0 \quad \cdots \quad 0}_{\ell_1} & \end{array} \tag{13}$$

occurs [i.e., a special case of Eq. (11)] and $Y_{p-1}=1$ if the event of Eq. (11) occurs with $i=p-1$. Also for $i \geqslant p+n_1-\ell_1$ configurations of the form Eq. (11) cannot occur since they necessarily specify ℓ_1+1 fibers, which cannot be accommodated to the right of the starting fiber of the configuration. Observe also that our special assignments $Z_{p-2}=Z_{p-1}=1$ enable us to treat the special configurations associated with the left boundary as also being configurations of the form Eq. (11).

If we set $\lambda_1=\mathbf{E}[T]=\Sigma_{i=p}^{p+n_1-1}\text{Prob}\{Y_i=1\}$, we obtain

$$\lambda_1(n_1)=(n_1-\ell_1)(\ell_1\alpha^{\ell_1}\beta_1^2)(\alpha+\beta_1)^{n_1-(\ell+2)} \times\left\{1+O\left(\frac{1}{n_1-\ell_1}\right)\right\}. \tag{14}$$

Then from Eq. (A3) we approximately have $\text{Prob}\{T=0\} \approx \exp(-\lambda_1)$ with an error $b_1+b_2+b_3$ whose magnitude we presently bound. We first choose $J_i=\{j:|j-i| \leqslant \ell_1+1\}$ to be the neighborhood of dependence of fiber *i*. This choice for J_i gives $b_3=0$ because then Y_i and $\{Y_j: j \notin J_i\}$ are independent as there are no common fibers involved between them. Since V_i depends only on $\{Y_j: j \notin J_i\}$, Y_i and V_i are independent and therefore $b_3=0$. Also from Eq. (A3) we have for b_1

$$b_1 \leqslant \min(1,1/\lambda_1)2(n_1-\ell_1)(\ell_1+1)[\lambda_1/(n_1-\ell_1)]^2 = \min(1,1/\lambda_1)2(\ell_1+1)\frac{\lambda_1^2(n_1)}{(n_1-\ell_1)}. \tag{15}$$

Here we have multiplied by only the factor $n_1-\ell_1$ because $p_ip_j=0$, when either $i>n_1-\ell_1$ or $j>n_1-\ell_1-1$, or both.

Bounding b_2 in Eq. (A3) requires finding pairs of failure configurations such that $Y_iY_j=1$ for $j \in J_i$. For $0 \leqslant s<\ell_1$, we have $Y_iY_j=1$ only for a configuration of the form

$$\begin{array}{ccccccccc} i & & j & & & & & & \\ & & \downarrow & & & & \downarrow & & \\ 1 & \underbrace{0 \quad \cdots \quad 0}_{0\leq s<\ell_1} & 1 & \underbrace{0 \quad \cdots \quad 0}_{\ell_1-s} & & \underbrace{0 \quad \cdots \quad 0}_{0\leq t<s} & 1 & \underbrace{0 \quad \cdots \quad 0}_{s-t} & \\ & \underbrace{\qquad\qquad\qquad\qquad}_{Y_i} & & & & & & & \\ & & \underbrace{\qquad\qquad\qquad\qquad\qquad\qquad\qquad\qquad}_{Y_j} & & & & & & \end{array} \tag{16}$$

and for fixed *s*, this has probability $s\beta_1^3\alpha^{\ell_1+s}(\alpha+\beta_1)^{n_1-(\ell_1+s+3)}$ so that

$$\sum_{s=0}^{\ell_1-1}\mathbf{E}[Y_iY_{i+s+1}] \leqslant \sum_{s=0}^{\ell_1-1} s\beta_1^3\alpha^{\ell_1+s}(\alpha+\beta_1)^{n_1-(\ell_1+s+3)} \leqslant \beta_1^3\alpha^{\ell_1}(\alpha+\beta_1)^{n_1-(\ell_1+3)}\sum_{s=0}^{\infty} s\gamma_1^s = \beta_1\alpha^{\ell_1+1}(\alpha+\beta_1)^{n_1-(\ell_1+2)} \tag{17}$$

when $i \leqslant p+n_1-\ell_1-1$ and is 0 otherwise. Also, when $i=p-2$ or $i=p-1$, the probability of those configurations is $\lambda_1 O(1/(n-\ell_1))$. Therefore,

$$b_2 \leqslant \min(1,1/\lambda_1)(n_1-\ell_1)\beta_1\alpha^{\ell_1+1}(\alpha+\beta_1)^{n_1-(\ell_1+2)} \leqslant \min(1,1/\lambda_1)\frac{2\alpha\lambda_1}{\ell_1\beta_1} \tag{18}$$

so that b_2 is $\lambda_1 O(1/\ell_1)$ as $\lambda_1 \downarrow 0$. For small λ_1, $\exp(-\lambda_1) \approx 1-\lambda_1$ so we may write the probability of failure of our 0-1 sub-bundle, $\mu_1(n_1)$, including the Chen-Stein error bound as

$$\mu_1(n_1)=(n_1-\ell_1)(\ell_1\alpha^{\ell_1}\beta_1^2)(\alpha+\beta_1)^{n_1-(\ell_1+2)} \times\left\{1\pm O\left(\frac{1}{\ell_1}+\frac{1}{n_1-\ell_1}\right)\right\}. \tag{19}$$

Anticipating the pattern that will emerge from the 0-1-2 and 0-1-2-3 calculations in Secs. II C and II D we rewrite this as

$$\mu_1(n_1)=(n_1-\ell_1)C_0\ell_1\alpha^{\ell_1}(\alpha+\beta_1)^{n_1-\ell_1} \times\left\{1\pm O\left(\frac{1}{\ell_1}+\frac{1}{n_1-\ell_1}\right)\right\} \tag{20}$$

where

$$C_0=\frac{\beta_1^2}{(\alpha+\beta_1)^2}=(1-\gamma_1)^2.$$

C. Strength of a 0-1-2 sub-bundle

The next step toward an approximate formula for the probability of failure of a general 0-1-2-$\cdots$-r sub-bundle, for $r\geqslant 2$, is the evaluation of the failure probability of a 0-1-2 sub-bundle, i.e., one whose fibers have $Z_i=2_0$.

We let $I_2=\{p,p+1,\ldots,p+n_2-1\}\subset I$ index a sub-bundle for some $p\leqslant n-n_2+1$ such that $Z_i=2_0$ for $i\in I_2$. Let Z_i be distributed as stated in Sec. II A. As in the case of the 0-1 sub-bundle, set $Z_{p-2}=Z_{p-1}=2$ for fictitious fibers at positions $p-2$ and $p-1$ to simplify the consideration of boundary effects. Then the sub-bundle indexed by I_2 fails if and only if the sub-bundle indexed by $I_2\cup\{p-2,p-1\}$ fails. Also let $n_2\geqslant\ell_2$.

Our procedure for approximating the failure probability of this sub-bundle is similar to that of the 0-1 sub-bundle, though it is more complicated due to the much larger number of possible failure configurations. We begin by defining failure configurations in the 0-1-2 sub-bundle in Sec. II C 1 and in Sec. II C 2 we evaluate their probabilities. Appendix C is concerned with bounding the Poisson approximation error $b_1+b_2+b_3$.

1. Failure configurations

The simplest failure configurations of the 0-1-2 sub-bundle are direct extensions of Eq. (11),

$$\begin{array}{c} i \qquad\qquad \downarrow \\ 2_1\ \underbrace{0\ \cdots\ 0}_{0\leq s<\ell_1}\ 2\ \underbrace{0\ \cdots\ 0}_{\ell_2-s} \end{array} \tag{21}$$

and

$$\begin{array}{c} i \qquad\qquad \downarrow \\ 2\ \underbrace{0\ \cdots\ 0}_{\ell_1\leq s<\ell_2}\ 2\ \underbrace{0\ \cdots\ 0}_{\ell_2-s}. \end{array} \tag{22}$$

In scanning the 0-1-2 sub-bundle from left to right, if either of these configurations is found we set $Y_i=1$ and consider the sub-bundle failed.

In addition to these direct extensions, there are configurations in which a pressured fiber with $Z_i=2$ is overloaded to failure by the earlier failure of a nearby 0-1 sub-bundle. In these configurations, we denote

$$\underbrace{1_0\ \cdots\ 1_0\ \langle 0\text{-}1\rangle\ 1_0\ \cdots\ 1_0}_{\ell_2-s}$$

to be a failing 0-1 sub-bundle with ℓ_2-s fibers and L is taken as a positive integer such that $L<\ell_1\wedge\ell_2-(\ell_1+1)$. Also, $\langle 0\text{-}1\rangle$ denotes the 0-1 failure configuration, Eq. (11). (It turns out later that optimally $L=-\log_{\gamma_1}\{\min[\ell_1,\ell_2-(\ell_1+1)]\}$.) Some configurations to consider are therefore

$$\begin{array}{c} i \qquad\qquad\qquad\qquad \downarrow \\ 2_1\ \underbrace{0\ \cdots\ 0}_{0\leq s<L}\ 2\ \underbrace{1_0\ \cdots\ 1_0\ \langle 0\text{-}1\rangle\ 1_0\ \cdots\ 1_0}_{\ell_2-s}, \end{array} \tag{23}$$

$$\begin{array}{c} i \qquad\qquad\qquad\qquad \downarrow \\ 2_1\ \underbrace{0\ \cdots\ 0}_{L\leq s<\ell_1\wedge(\ell_2-(\ell_1+1))}\ 2\ \underbrace{1_0\ \cdots\ 1_0\ \langle 0\text{-}1\rangle\ 1_0\ \cdots\ 1_0}_{\ell_2-s}, \end{array} \tag{24}$$

$$\begin{array}{c} i \qquad\qquad\qquad\qquad \downarrow \\ 2\ \underbrace{0\ \cdots\ 0}_{\ell_1\leq s<\ell_2-(\ell_1+1)}\ 2\ \underbrace{1_0\ \cdots\ 1_0\ \langle 0\text{-}1\rangle\ 1_0\ \cdots\ 1_0}_{\ell_2-s}, \end{array} \tag{25}$$

$$\begin{array}{c} i \qquad\qquad\qquad\qquad\qquad\qquad \downarrow \\ 2_1\ \underbrace{0\ \cdots\ 0}_{0\leq t<s}\ 2\ \underbrace{1_0\ \cdots\ 1_0\ \langle 0\text{-}1\rangle\ 1_0\ \cdots\ 1_0}_{\ell_2-s}\ 2\ \underbrace{0\ \cdots\ 0}_{1\leq s<L}, \end{array} \tag{26}$$

$$\overset{i}{\underset{}{}}\qquad\qquad\overset{\downarrow}{\underset{}{}}$$
$$2\,\underbrace{1_0\cdots 1_0\,\langle 0\text{-}1\rangle\,1_0\cdots 1_0}_{\ell_2-s}\,2\,\underbrace{0\quad\cdots\quad 0}_{L\le s<\ell_2-(\ell_1+1)}, \tag{27}$$

$$\overset{i}{\underset{}{}}\qquad\qquad\overset{\downarrow}{\underset{}{}}$$
$$2\,\underbrace{1_0\cdots 1_0\,\langle 0\text{-}1\rangle\,1_0\cdots 1_0}_{\ell_1+2\le s<\ell_2-(\ell_1+1)}\,2\,\underbrace{1_0\cdots 1_0\,\langle 0\text{-}1\rangle\,1_0\cdots 1_0}_{\ell_2-s}, \tag{28}$$

where, in this last configuration, failure of the 0-1-2 sub-bundle occurs by failing a pressured 2 fiber, which requires the failure of two 0-1 sub-bundles, one on each side.

Failure configurations of a 0-1-2 sub-bundle need not have a 2 fiber at the pressured position. The following are valid failure configurations, which are not counted by the failure configurations listed thus far. In these cases, we take the 0-1 sub-bundle's failure configuration as the pressured element, and thus can have

$$\overset{i}{\underset{}{}}\qquad\qquad\overset{\downarrow}{\underset{}{}}$$
$$\underbrace{0\quad\cdots\quad 0}_{\ell_2-\ell_1-s-1}\,2\,\underbrace{1_0\cdots 1_0}_{0\vee(\ell_2-2\ell_1)\le s<\ell_2-(\ell_1+2)}\,\underbrace{\langle 0\text{-}1\rangle\;1_0\;\cdots\;1_0}_{\ell_2-s} \tag{29}$$

and

$$\overset{i}{\underset{}{}}\qquad\overset{\downarrow}{\underset{}{}}$$
$$2\,\underbrace{1_0\cdots 1_0}_{\ell_2-(\ell_1+2)\le s<\ell_2}\,\underbrace{\langle 0\text{-}1\rangle}_{\ell_1+2} \tag{30}$$

and, indeed, a sufficiently long failing 0-1 sub-bundle can double as a failing 0-1-2 sub-bundle, namely,

$$\overset{i}{\underset{}{}}\qquad\overset{\downarrow}{\underset{}{}}$$
$$\underbrace{1_0\quad\cdots\quad 1_0}_{\ell_2}\,\underbrace{\langle 0\text{-}1\rangle}_{\ell_1+2}. \tag{31}$$

A few remarks about these configurations are in order. First, we claim that the above collection of failure configurations is exhaustive in that a failing sub-bundle of $Z_i=2_0$, $i\in I_2$, fibers must contain at least one of the configurations listed above. Second, not all the above listed configurations are possible for arbitrary ℓ_1 and ℓ_2. If, for instance $\ell_1>\ell_2-(\ell_1+1)$, the configurations Eq. (25) and Eq. (28) are impossible. Third, notice that in configurations Eq. (26) and Eq. (29) we specify certain fibers to the left of fiber *i*, whereas in the other configurations we do not. This is done to reduce overlap between configurations so that the dominating part of the Poisson approximation error, b_2, can be kept small in comparison to the probability of bundle failure. For instance, without fibers to the left of fiber *i* in Eq. (26), we have the configuration $2\,1_0\cdots 1_0\,2\,0\cdots 0$ which may overlap Eq. (23) as

$$\overset{i}{\underset{}{}}\qquad\overset{j}{\underset{}{}}\qquad\qquad\overset{\downarrow}{\underset{}{}}\qquad\qquad\overset{\downarrow}{\underset{}{}}$$
$$2_1\,\underbrace{0\quad\cdots\quad 0}_{0\le s_1<L}\,2\,\underbrace{1_0\cdots 1_0\,\langle 0\text{-}1\rangle\,1_0\cdots 1_0}_{\ell_2-s_1}\,\underbrace{1_0\cdots 1_0}_{\ell_2-s_2+s_1}\,2\,\underbrace{0\quad\cdots\quad 0}_{1\le s_2<L}$$

and this results in b_2 being of the order of the probability being estimated. Using the methods of the next section, the probability of this event may be seen to be of order comparable to the probability of occurrence of either Eq. (23) or Eq. (26), which dominate the probability being estimated. Since a tight error bound is desired, this situation is to be avoided.

2. Failure probability

The probability of occurrence of any of the various failure configurations listed in Sec. II C 1 depends on $i\in I_2$. Since each configuration specifies at least ℓ_2+2 fibers to the right of fiber *i*,

$$Y_i=0 \quad \text{for } i\ge p+n_2-\ell_2-1,$$

that is, by definition the sub-bundle cannot be failed. Thus we let $L \leqslant i < p+n_2-\ell_2-1$, and evaluate the probability of occurrence of configurations Eq. (23) and Eq. (26). We show that these are the dominant failure configurations in that their probability of occurrence is of higher order than that of all other failure configurations listed in Sec. II C 1.

From the configuration Eq. (23) and Eq. (20) we have

$$\begin{aligned}\text{Prob}\{\text{Eq. (23)}\} &= (\beta_1+\beta_2)\beta_2(\alpha+\beta_1+\beta_2)^{n_2-(\ell_2+2)}\sum_{s=0}^{L-1}\alpha^s\mu_1(\ell_2-s)\\ &= \frac{(\alpha+\beta_1)(\beta_1+\beta_2)\beta_2}{\beta_1(\alpha+\beta_1+\beta_2)^2}\mu_1(\ell_2)(\alpha+\beta_1+\beta_2)^{n_2-\ell_2}\{1\pm O(\gamma_1^L)\},\end{aligned} \tag{32}$$

where γ_j is defined in Eq. (10). Also, for the configuration Eq. (26) we have

$$\begin{aligned}\text{Prob}\{\text{Eq. (26)}\} &= (\beta_1+\beta_2)\beta_2^2\sum_{s=1}^{L-1}\sum_{t=0}^{s-1}\alpha^{s+t}\mu_1(\ell_2-s)(\alpha+\beta_1+\beta_2)^{n_2-(\ell_2+t+3)}\\ &= \frac{\beta_2^2\alpha(\alpha+\beta_1)(\beta_1+\beta_2)}{\beta_1(\alpha+\beta_1+\beta_2)^2\{(\alpha+\beta_1)(\beta_1+\beta_2)+\alpha\beta_1\}}\mu_1(\ell_2)(\alpha+\beta_1+\beta_2)^{n_2-\ell_2}\{1\pm O(\gamma_1^L)\}.\end{aligned} \tag{33}$$

Adding the disjoint probabilities Eq. (32) and Eq. (33) we obtain

$$\text{Prob}\{\text{Eq. (23)}\cup\text{Eq. (26)}\} = \frac{\beta_2(\alpha+\beta_1)(2\alpha+\beta_1)(\beta_1+\beta_2)^2}{\beta_1(\alpha+\beta_1+\beta_2)^2\{(\alpha+\beta_1)(\beta_1+\beta_2)+\alpha\beta_1\}}\mu_1(\ell_2)(\alpha+\beta_1+\beta_2)^{n_2-\ell_2}\{1\pm O(\gamma_1^L)\}. \tag{34}$$

It is shown in Eq. (B7) of Appendix B that the sum of the failure probability contributions of failure events besides Eq. (23) and Eq. (26), listed in Sec. II C 1, is of diminished order

$$\text{Prob}\{\text{Eq. (23)}\cup\text{Eq. (26)}\}\times O\left(\gamma_1^L+\frac{\ell_1\{(\ell_2-2\ell_1)\vee 0\}^3}{\ell_2-\ell_1}\gamma_1^{\ell_1}\right). \tag{35}$$

Furthermore, it is shown there that the probability contribution of the boundary configurations with $p \leqslant i \leqslant p+L$ is of diminished order

$$\text{Prob}\{\text{Eq. (23)}\cup\text{Eq. (26)}\}O\left(\frac{L}{n_2-\ell_2}\right), \tag{36}$$

where $0 \leqslant L \leqslant \ell_1$. In the asymptotic analysis, the parameter L will be given special properties below.

Setting $\lambda_2 = \mathbf{E}[T] = \Sigma_{i=p}^{p+n_2-1}\text{Prob}\{Y_i=1\}$, we have from Eq. (34), Eq. (35), and Eq. (36) that

$$\begin{aligned}\lambda_2(n_2) &= (n_2-\ell_2)C_1\mu_1(\ell_2)(\alpha+\beta_1+\beta_2)^{n_2-\ell_2}\\ &\times\left\{1\pm O\left(\gamma_1^L+\frac{\ell_1\{(\ell_2-2\ell_1)\vee 0\}^3}{\ell_2-\ell_1}\gamma_1^{\ell_1}+\frac{L}{n_2-\ell_2}\right)\right\},\end{aligned} \tag{37}$$

where

$$C_1 = \frac{(\gamma_1-\gamma_2)(1+\gamma_1)(1-\gamma_2)^2}{\gamma_1(1-\gamma_1)(1-\gamma_1\gamma_2)}.$$

Choosing $L = \lceil -\log_{\gamma_1}[\ell_1 \wedge (\ell_2-\ell_1)]\rceil$, we can make the error term close to its smallest value with respect to varying L so that

$$\begin{aligned}\lambda_2(n_2) &= (n_2-\ell_2)C_1\mu_1(\ell_2)(\alpha+\beta_1+\beta_2)^{n_2-\ell_2}\\ &\times\left\{1\pm O\left(\frac{\ell_1\{(\ell_2-2\ell_1)\vee 0\}^3}{\ell_2-\ell_1}\gamma_1^{\ell_1}+\frac{\lceil -\log_{\gamma_1}[\ell_1\wedge(\ell_2-\ell_1)]\rceil}{n_2-\ell_2}\right)\right\}.\end{aligned} \tag{38}$$

As in the 0-1 case, we still need to compute the Chen-Stein error term $b_1+b_2+b_3$ arising from the Poisson approximation of the dependent, bundle failure event process Y_i. We show in Appendix C that this error is of order $\lambda_2 O(\gamma_1^L)$ and therefore is smaller in order than the error generated by omitting all but the two most dominant configurations and boundary configuration terms.

Thus, the probability of failure of a 0-1-2 sub-bundle, accounting for both boundary and Poisson approximation errors, is

$$\begin{aligned}\mu_2(n_2) &= (n_2-\ell_2)C_1\mu_1(\ell_2)(\alpha+\beta_1+\beta_2)^{n_2-\ell_2}\\ &\times\left\{1\pm O\left(\frac{\ell_1\{(\ell_2-2\ell_1)\vee 0\}^3}{\ell_2-\ell_1}\gamma_1^{\ell_1}+\frac{1}{\ell_1}+\frac{1}{\ell_2-\ell_1}+\frac{\lceil -\log_{\gamma_1}[\ell_1\wedge(\ell_2-\ell_1)]\rceil}{n_2-\ell_2}\right)\right\}\end{aligned} \tag{39}$$

where

$$C_1 = \frac{\beta_2(\alpha+\beta_1)(2\alpha+\beta_1)(\beta_1+\beta_2)^2}{\beta_1(\alpha+\beta_1+\beta_2)^2\{(\alpha+\beta_1)(\beta_1+\beta_2)+\alpha\beta_1\}} = \frac{(\gamma_1-\gamma_2)(1+\gamma_1)(1-\gamma_2)^2}{\gamma_1(1-\gamma_1)(1-\gamma_1\gamma_2)}.$$

D. Strength of a 0-1-2-3 sub-bundle

Extending the previous setup to 0-1-2-3 sub-bundles, we let $I_3 = \{p-2, p-1, p, p+1, \ldots, p+n_3-1\} \subset I$ for some $p \leqslant n-n_3+1$ such that $Z_i = 3_0$ for $i \in I_3$. Let Z_i be distributed as described in Sec. II A except that $Z_{p-2} = Z_{p-1} = 2_1$. Also let $n_3 \geqslant \ell_3$.

Let L be as defined in Sec. II C 1 and let us denote a failing 0-1-2 sub-bundle $\ell_3 - s$ fibers long by

$$\underbrace{2_0 \cdots 2_0 \langle 0\text{-}1\text{-}2\rangle 2_0 \cdots 2_0}_{\ell_3 - s}.$$

Configuration Eq.(23) then generalizes to

$$\overset{i}{3_1} \underbrace{0 \cdots 0}_{0 \le s < L} \overset{\downarrow}{3} \underbrace{2_0 \cdots 2_0 \langle 0\text{-}1\text{-}2\rangle 2_0 \cdots 2_0}_{\ell_3 - s} \tag{40}$$

and

$$\overset{i}{3_1} \underbrace{0 \cdots 0}_{0 \le s < L} \overset{\downarrow}{3} \underbrace{1_0 \cdots 1_0 \langle 0\text{-}1\rangle 1_0 \cdots 1_0}_{\ell_3 - s} \tag{41}$$

and configuration Eq. (26) generalizes to

$$3_1 \underbrace{0 \cdots 0}_{0 \le t < s} \overset{i}{3} \underbrace{2_0 \cdots 2_0 \langle 0\text{-}1\text{-}2\rangle 2_0 \cdots 2_0}_{\ell_3 - s} \overset{\downarrow}{3} \underbrace{0 \cdots 0}_{1 \le s < L} \tag{42}$$

and

$$3_1 \underbrace{0 \cdots 0}_{0 \le t < s} \overset{i}{3} \underbrace{1_0 \cdots 1_0 \langle 0\text{-}1\rangle 1_0 \cdots 1_0}_{\ell_3 - s} \overset{\downarrow}{3} \underbrace{0 \cdots 0}_{1 \le s < L} \tag{43}$$

The probabilities for these events (we do not write explicit error bounds here) sum to

$$\text{Prob}\{\text{Eq. (40)}\} = (\beta_1+\beta_2+\beta_3)\beta_3(\alpha+\beta_1+\beta_2+\beta_3)^{n_3-(\ell_3+2)} \sum_{s=0}^{L-1} \alpha^s \mu_2(\ell_3 - s)$$
$$= \frac{(\alpha+\beta_1+\beta_2)(\beta_1+\beta_2+\beta_3)\beta_3}{(\beta_1+\beta_2)(\alpha+\beta_1+\beta_2+\beta_3)^2} \mu_2(\ell_3)(\alpha+\beta_1+\beta_2+\beta_3)^{n_3-\ell_3}, \tag{44}$$

and

$$\text{Prob}\{\text{Eq. (41)}\} = (\beta_1+\beta_2+\beta_3)\beta_3(\alpha+\beta_1+\beta_2)^{n_3-(\ell_3+2)} \sum_{s=0}^{L-1} \alpha^s \mu_1(\ell_3 - s)$$
$$= \frac{(\alpha+\beta_1)(\beta_1+\beta_2+\beta_3)\beta_3}{\beta_1(\alpha+\beta_1+\beta_2+\beta_3)^2} \mu_1(\ell_3)(\alpha+\beta_1+\beta_2+\beta_3)^{n_3-\ell_3}. \tag{45}$$

Since

$$\frac{\mu_1(\ell_3)}{\mu_2(\ell_3)} = O\left\{ \frac{\ell_3 - \ell_1}{(\ell_3-\ell_2)(\ell_2-\ell_1)} \left(\frac{\alpha+\beta_1}{\alpha+\beta_1+\beta_2} \right)^{\ell_3-\ell_2} \right\} = O\left\{ \left(\frac{1}{\ell_3-\ell_2} + \frac{1}{\ell_2-\ell_1} \right) \left(\frac{\gamma_2}{\gamma_1} \right)^{\ell_3-\ell_2} \right\},$$

the probability given by Eq. (44) dominates that given by Eq. (45). Next we find that

$$\text{Prob}\{\text{Eq. (42)}\} = (\beta_1+\beta_2+\beta_3)\beta_3^2 \sum_{s=1}^{L-1} \sum_{t=0}^{s-1} \alpha^{s+t} \mu_2(\ell_2 - s)(\alpha+\beta_1+\beta_2+\beta_3)^{n_3-(\ell_3+3+t)}$$
$$= \frac{\beta_3^2 \alpha(\beta_1+\beta_2+\beta_3)(\alpha+\beta_1+\beta_2)}{(\beta_1+\beta_2)\{(\alpha+\beta_1+\beta_2)(\beta_1+\beta_2+\beta_3)+\alpha(\beta_1+\beta_2)\}} \mu_2(\ell_3)(\alpha+\beta_1+\beta_2+\beta_3)^{n_3-(\ell_3+2)} \tag{46}$$

and

$$\text{Prob}\{\text{Eq. (43)}\}=(\beta_1+\beta_2+\beta_3)\beta_3^2\sum_{s=1}^{\ell-1}\sum_{t=0}^{s-1}\alpha^{s+t}\mu_1(\ell_3-s)(\alpha+\beta_1+\beta_2+\beta_3)^{n_3-(\ell_3+3+t)}$$

$$=\frac{\beta_3^2\alpha(\beta_1+\beta_2+\beta_3)(\alpha+\beta_1)}{\beta_1\{(\alpha+\beta_1)(\beta_1+\beta_2+\beta_3)+\alpha\beta_1\}}\mu_1(\ell_3)(\alpha+\beta_1+\beta_2+\beta_3)^{n_3-(\ell_2+2)}. \tag{47}$$

Equation (47) can be seen to be of smaller order of magnitude than Eq. (46), exactly as Eq. (44) is seen to dominate Eq. (45). Also, adding the probabilities in Eq. (44) and Eq. (46) gives

$$\text{Prob}\{\text{Eq. (40)}\cup\text{Eq. (42)}\}=\frac{\beta_3(\alpha+\beta_1+\beta_2)(2\alpha+\beta_1+\beta_2)(\beta_1+\beta_2+\beta_3)^2}{(\beta_1+\beta_2)\{(\alpha+\beta_1+\beta_2)(\beta_1+\beta_2+\beta_3)+\alpha(\beta_1+\beta_2)\}}\mu_2(\ell_3)(\alpha+\beta_1+\beta_2+\beta_3)^{n_3-(\ell_3+2)}. \tag{48}$$

We must also consider configurations of the form

$$\begin{matrix} & i & & & & & \downarrow & \\ 3 & \underbrace{2_0\ \cdots\ 2_0\ \langle 0\text{-}1\text{-}2\rangle\ 2_0\ \cdots\ 2_0}_{\ell_2+2\le s<\ell_3-(\ell_2+1)} & 3 & \underbrace{2_0\ \cdots\ 2_0\ \langle 0\text{-}1\text{-}2\rangle\ 2_0\ \cdots\ 2_0}_{\ell_3-s} & , & & & \end{matrix} \tag{49}$$

which have probability

$$\text{Prob}\{\text{Eq. (49)}\}=\beta_3^2\sum_{s=\ell_2+2}^{\ell_3-(\ell_2+2)}\mu_2(s)\mu_2(\ell_3-s)$$

$$=\text{Prob}\{\text{Eq. (40)}\cup\text{Eq. (42)}\}O\left(\frac{\ell_1(\ell_2-\ell_1)\{(\ell_3-2\ell_2)\vee 0\}^3}{\ell_3-\ell_2}\gamma_1^{\ell_1}\left(\frac{\gamma_2}{\gamma_1}\right)^{\ell_2}\right). \tag{50}$$

In a manner similar to the 0-1-2 case, we can show that all other failure configurations of a 0-1-2-3 bundle are dominated by the configurations described by Eq. (40) and Eq. (42). Accounting for the discrepancy in the probability of Eq. (42) when $p\leqslant i<p+L$ exactly as in the 0-1-2 bundle, for $\lambda_3=\mathbf{E}[T]=\Sigma_{i=p}^{p+n_3-1}\text{Prob}\{Y_i=1\}$ we finally have the result

$$\lambda_3(n_3)=(n_3-\ell_3)[C_2\mu_2(\ell_3)](\alpha+\beta_1+\beta_2+\beta_3)^{n_3-\ell_3}\left\{1\pm O\left(\frac{1}{\ell_1}+\frac{1}{\ell_2-\ell_1}+\frac{L}{\ell_3-\ell_2}+\frac{L}{n_3-\ell_3}+\frac{\ell_1\{(\ell_2-2\ell_1)\vee 0\}^3}{\ell_2-\ell_1}\gamma_1^{\ell_1}\right.\right.$$

$$\left.\left.+\frac{\ell_1(\ell_2-\ell_1)\{(\ell_3-2\ell_2)\vee 0\}^3}{\ell_3-\ell_2}\gamma_1^{\ell_1}\left(\frac{\gamma_2}{\gamma_1}\right)^{\ell_2}\right)\right\} \tag{51}$$

where

$$C_2=\frac{\beta_3(\alpha+\beta_1+\beta_2)(2\alpha+\beta_1+\beta_2)(\beta_1+\beta_2+\beta_3)^2}{(\beta_1+\beta_2)(\alpha+\beta_1+\beta_2+\beta_3)^2\{(\alpha+\beta_1+\beta_2)(\beta_1+\beta_2+\beta_3)+\alpha(\beta_1+\beta_2)\}}=\frac{(\gamma_2-\gamma_3)(1+\gamma_2)(1-\gamma_3)^2}{\gamma_2(1-\gamma_2)(1-\gamma_2\gamma_3)}.$$

The Poisson approximation error can be bounded exactly as in the 0-1-2 case. It turns out to be of the order of the error term in Eq. (51) and, including that as well, we can take $\mu_3(n_3)=\lambda_3(n_3)$ as the probability of failure of the 0-1-2-3 sub-bundle.

E. Strength of a 0-1-2-⋯-*r* sub-bundle

The above steps generalize from a 0-1-2-⋯-$(j-1)$ sub-bundle to a 0-1-2-⋯-j sub-bundle and can be carried out indefinitely. For the 0-1-2-⋯-$j, j\geqslant 2$ sub-bundle, which is n_j fibers long, the dominant failure configurations are

$$\begin{matrix} & i & & & & \downarrow & \\ j_1 & \underbrace{0\ \cdots\ 0}_{0\le s<L} & j & \underbrace{(j-1)_0\ \cdots\ (j-1)_0\ \langle 0\text{-}1\text{-}2\text{-}\cdots\text{-}(j-1)\rangle\ (j-1)_0\ \cdots\ (j-1)_0}_{\ell_j-s} & & \end{matrix} \tag{52}$$

and

$$\underset{}{\overset{i}{}}$$

$$j_1 \underbrace{0 \cdots 0}_{0\le t<s}\, j \underbrace{(j-1)_0 \cdots (j-1)_0 \langle 0\text{-}1\text{-}\cdots\text{-}(j-1)\rangle (j-1)_0 \cdots (j-1)_0}_{\ell_j - s}$$

$$\downarrow$$

$$\cdots\, j \underbrace{0 \cdots 0}_{1\le s<L}, \tag{53}$$

and evaluating their probabilities as before, we have

$$\mu_j(n_j) = (n_j-\ell_j)[C_{j-1}\mu_{j-1}(\ell_j)](\alpha+\beta_1+\cdots+\beta_j)^{n_j-\ell_j} \times\left\{1 \pm O\left(\frac{\lceil -\log_{\gamma_1}[\ell_1\wedge(\ell_2-\ell_1)]\rceil}{n_j-\ell_j} + \frac{\ell_1(\ell_2-\ell_1)\cdots(\ell_{j-1}-\ell_{j-2})\{(\ell_j-2\ell_{j-1})\vee 0\}^3}{\ell_j-\ell_{j-1}} \times\gamma_1^{\ell_1}\left(\frac{\gamma_2}{\gamma_1}\right)^{\ell_2}\cdots\left(\frac{\gamma_{j-1}}{\gamma_{j-2}}\right)^{\ell_{j-1}}\right)\right\} \tag{54}$$

where

$$C_{j-1} = \frac{(\gamma_{j-1}-\gamma_j)(1+\gamma_{j-1})(1-\gamma_j)^2}{\gamma_{j-1}(1-\gamma_{j-1})(1-\gamma_j\gamma_{j-1})}.$$

This is the relation between the probability of failure of a 0-1-2-$\cdots$-j and a 0-1-2-$\cdots$-$j-1$ bundle and it brings out the hierarchical nature of the failure process.

Explicitly, at the largest scale, by substituting for μ_j, $j=1,2,\ldots,r-1$, and taking n_r to be n (i.e., for a given load the next largest bundle in the hierarchy is the full bundle) we obtain

$$\mu_r(n) = C_0C_1C_2\cdots C_{r-1}\ell_1(\ell_2-\ell_1)(\ell_3-\ell_2)\cdots(\ell_r-\ell_{r-1}) \times(n-\ell_r)\alpha^{\ell_1}(\alpha+\beta_1)^{\ell_2-\ell_1}\cdots(\alpha+\beta_1 +\cdots\beta_{r-1})^{\ell_r-\ell_{r-1}}(1\pm\varepsilon), \tag{55}$$

where

$$\varepsilon = O\left(\frac{\lceil -\log_{\gamma_1}[\ell_1\wedge(\ell_2-\ell_1)]\rceil}{(n-\ell_r)\wedge[\wedge_{j=1}^{r}(\ell_j-\ell_{j-1})]} + \underset{j=2}{\overset{r}{\vee}} \frac{\prod_{m=2}^{j}\{(\ell_{m-1}-\ell_{m-2})(\gamma_{m-1}/\gamma_{m-2})^{\ell_{m-1}}\}\{(\ell_j-2\ell_{j-1})\vee 0\}^3}{\ell_j-\ell_{j-1}}\right) \tag{56}$$

where terms involving $\ell_p, p\leqslant 0$, have been dropped. We have also used the identity $\alpha+\beta_1+\cdots+\beta_r=1$. The error term is greatly simplified if $\ell_j \leqslant 2\ell_{j-1}$ since the second term in Eq. (56) vanishes. Also note that

$$\prod_{j=1}^{r} C_{j-1} = (1-\gamma_1)(1-\gamma_r) \times\prod_{j=2}^{r}\frac{(\gamma_{j-1}-\gamma_j)(1+\gamma_{j-1})(1-\gamma_j)}{\gamma_{j-1}(1-\gamma_j\gamma_{j-1})}. \tag{57}$$

We have shown so far that the probability of failure of a bundle in the composite with discretely distributed fiber strengths is given by Eq. (55), and the dominant failure mode of this bundle, when the γ_j's and ℓ_j's are such that the error term ε in Eq. (56) is small, is that failure is initiated by the failure of a 0-1 sub-bundle, which causes the failure of a 0-1-2 sub-bundle, and so on (Fig. 2) until a 0-1-2-$\cdots$-r sub-bundle fails. The dominant failure mode *deduced* here is very similar to Smith's dominant failure mode valid only for large ρ which underlies Eq. (8); the ''fiber adjacent to a fiber break'' in Smith's argument corresponds to a ''sub-bundle encompassing a failed sub-bundle'' in the present calculation. We note, however, that this structure is unlike that of Newman *et al.*'s [28] hierarchical bundle model. We next use Eq. (55) to bound the failure probability of a large bundle whose fiber strengths are continuously distributed according to the power distribution $F(x)=x^\rho, 0\leqslant x\leqslant 1$, and will notice further similarities there between Smith's formula and the present formula.

III. BUNDLES WITH CONTINUOUSLY DISTRIBUTED FIBER STRENGTH

We now use Eq. (55) to estimate the strength distribution $G_n(x)$ of an n-fiber bundle under local load sharing and whose fiber strengths are distributed according to the power law

$$F(x)=x^{\rho}1_{[0\leqslant x\leqslant 1]}+1_{[x>1]}, \tag{58}$$

where ρ is the shape parameter of the distribution. To do so, we must discretize $F(x)$. For simplicity, we restrict the applied load per fiber to take on one of the discrete values

$$x_k=\frac{1}{K_{k^2c}}=\frac{1}{1+(k^2c/2)}, \quad k=0,1,2,\ldots, \tag{59}$$

where c is an arbitrary integer chosen sufficiently large, as described below. (Recall from Sec. II A that K_ℓ denotes the load concentration on a fiber adjacent to ℓ fiber breaks, and specifically that $K_\ell=1+\ell/2$ according to the assumption of idealized local load sharing.) According to Eq. (59), then, x_k refers to the smallest load which causes catastrophic bundle failure if k^2c breaks occur adjacent to some survivor. In other words, k^2c is the critical cluster size for load x_k [see text below Eq. (8)]. $x_1,x_2,x_3,\ldots,x_k,\ldots$ form a decreasing sequence of possible applied loads per fiber with limit zero. We will be interested in the asymptotic behavior of $G_n(x)$ when $x=x_k$ and k becomes large. For the time being, however, all the calculations up to the end of this section will treat k and x_k as fixed, where we keep in mind that k^2c is a "critical cluster size" associated with bundle loads from x_k up to x_{k-1}.

Given k and $F(x)$, we consider bounding distributions $\underline{F}_k(x)$ and $\overline{F}_k(x)$ defined as

$$\underline{F}_k(x)=F(K_u x_k)1_{[K_u x_k<x\leqslant K_v x_k]}+1_{[x>1]} \tag{60}$$

and

$$\overline{F}_k(x)=F(K_v x_k)1_{[K_u x_k\leqslant x<K_v x_k]}+1_{[x>1]}, \tag{61}$$

where $u=(j-1)^2c$, and $v=j^2c$ and $j=1,2,\ldots,k$ are chosen to satisfy the inequalities around x. Thus, for all x we have

$$\underline{F}_k(x)\leqslant F(x)\leqslant\overline{F}_k(x). \tag{62}$$

Figure 3 illustrates the power law distribution function for $\rho=1.5$ together with the bounding distribution functions based on $c=2$ and $k=3$. Thus there are three main "steps" in each bounding distribution, associated with $j=0,1,2,3$, and the lowest nonzero discrete fiber strength and discrete bundle load per fiber value is $x_3=0.1$.

We let $G_n(x)$, $\overline{G}_n(x)$, and $\underline{G}_n(x)$ be the bundle strength distributions corresponding to fiber strength distributions $F(x)$, $\overline{F}_k(x)$, and $\underline{F}_k(x)$, respectively. Given Eq. (62), it turns out that

$$\underline{G}_n(x)\leqslant G_n(x)\leqslant\overline{G}_n(x). \tag{63}$$

This can be seen by investigating realizations of fiber strength to construct a bundle and noting the monotonic, nondecreasing nature of stress concentrations on surviving fibers as fibers fail. For any realization ω_F

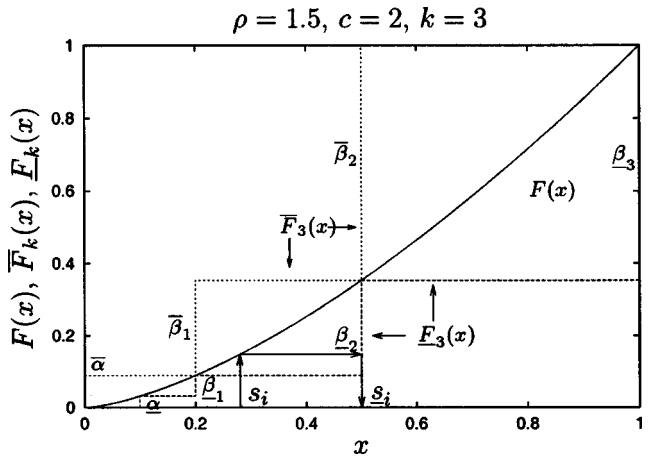

FIG. 3. An example of bounding a continuous power law distribution $F(x)$ by discrete $\overline{F}_k(x)$ and $\underline{F}_k(x)$. The continuous power law has $\rho=1.5$, and the discretization uses $k=3$ and $c=2$. This gives the lowest discrete fiber strength and bundle load per fiber value as $x_k=x_3=0.1$, which is where $\underline{F}_3(x)$ makes its first jump. Note that $k^2c=18$ is the critical cluster size for load x_k.

$=\{s_1,s_2,\ldots,s_n\}$ of i.i.d. fiber strengths drawn from $F(x)$ to form a bundle, we can construct $\omega_{\underline{F}}=\{\underline{s}_1,\underline{s}_2,\ldots,\underline{s}_n\}$, where

$$\underline{s}_i=1+\frac{c}{2}\left[\frac{2}{c}\sqrt{\frac{s_i}{x_k}-1}\right]^2, \quad i=1,2,\ldots,n, \tag{64}$$

to represent an i.i.d. realization drawn from $\underline{F}_k$. Figure 3 depicts the $s_i\rightarrow\underline{s}_i$ transformation given in Eq. (64). We see that every bundle realization ω_F is weaker than its corresponding $\omega_{\underline{F}}$, since, for each i, the fiber strength $\underline{s}_i$ in $\omega_{\underline{F}}$ is at least as strong as the corresponding s_i in ω_F. Hence, the failure probability of the set of all $\omega_{\underline{F}}$'s, $\underline{G}_n(x)$, must be smaller for every x than the corresponding $G_n(x)$. By a similar argument, it can also be shown that $\overline{G}_n(x)\geqslant G_n(x)$.

For the discrete fiber distribution function $\underline{F}_k(x)$ and for fixed k we have the probability masses

$$\underline{\alpha}=x_k^{\rho},$$

$$\underline{\beta}_j=(K_{j^2c}x_k)^{\rho}-(K_{(j-1)^2c}x_k)^{\rho}, \quad j=1,\ldots,k, \tag{65}$$

for the k possible discrete fiber strengths. Similarly, corresponding to $\overline{F}_k(x)$, we have

$$\overline{\alpha}=(K_c x_k)^{\rho},$$

$$\overline{\beta}_j=(K_{(j+1)^2c}x_k)^{\rho}-(K_{j^2c}x_k)^{\rho}, \quad j=1,\ldots,k-1. \tag{66}$$

Also, we have the critical fiber failure sequence lengths $\ell_j=cj^2$, $j=1,2,\ldots,k$, corresponding to $\underline{F}_k$, and $\ell_j=cj^2$, $j=1,\ldots,k-1$, corresponding to $\overline{F}_k$, and these actually determine the α and β probabilities and discrete strengths in the bounding distributions $\overline{F}_k$ and $\underline{F}_k$.

This choice for ℓ_j maximizes $\mu_k(n)=\underline{G}_n(x_k)$; i.e., of all possible m in the power form $\ell_j=cj^m$, the choice $m=2$

satisfies $\partial \log \mu_k / \partial \ell_j = 0$ most closely, for $j=1,\ldots,k$. Similarly, $\ell_j = cj^2, j=1,\ldots,k-1$, minimizes $\overline{G}_n(x_k)$. Thus, the choice of ℓ_j is such that $\underline{G}_n(x_k)$ and $\overline{G}_n(x_k)$ are nearly the tightest possible bounds on $G_n(x_k)$. With this choice of ℓ_j, we also see for both $\underline{F}_k(x)$ and $\overline{F}_k(x)$ that the error term Eq. (56) is $O(1/c)$.

We now apply Eq. (55) to compute the probability of failure of a 0-1-2-$\cdots$-k bundle $\underline{G}_n(x_k)$ whose fiber strengths are distributed according to $\underline{F}_k(x)$ and the applied bundle load per fiber is x_k. Observe that in this case

$$\gamma_j = K_{j^2c}^{-\rho}, \tag{67}$$

so the first product in Eq. (55) becomes

$$\begin{aligned}\prod_{j=1}^{k} C_{j-1} &= \left(1-\frac{1}{K_1^\rho}\right)\left(1-\frac{1}{K_r^\rho}\right) \\ &\quad \times \prod_{j=2}^{k} \frac{(1/K_{j-1}^\rho - 1/K_j^\rho)(1+1/K_{j-1}^\rho)(1-1/K_j^\rho)}{(1/K_{j-1}^\rho)(1-1/K_{j-1}^\rho K_j^\rho)} \\ &\approx \prod_{j=1}^{k}\left[1-\left(\frac{K_{j-1}}{K_j}\right)^\rho\right] = \prod_{j=1}^{k}\left[1-\left(\frac{c(j-1)^2+2}{cj^2+2}\right)^\rho\right] \\ &\approx \prod_{j=1}^{k}\left[1-\left(1-\frac{1}{j}\right)^{2\rho}\right]. \end{aligned} \tag{68}$$

To further simplify Eq. (68) we note that

$$1-\left(1-\frac{1}{j}\right)^{2\rho} \approx \begin{cases} 2\rho/j & \text{for } j > \lceil 3\rho \rceil, \\ \exp(-e^{-2\rho/j}) & \text{for } j \leqslant \lceil 3\rho \rceil, \end{cases} \tag{69}$$

where we have picked the transition point from one form to the other by comparing the numerical values of each form on the right side with the form on the left side. Then

$$\prod_{j=1}^{k} C_{j-1} \approx \prod_{j=1}^{k}\left[1-\left(1-\frac{1}{j}\right)^{2\rho}\right] \approx \Phi(\rho)\frac{(2\rho)^k}{k!}, \tag{70}$$

where

$$\begin{aligned}\Phi(\rho) &= \prod_{j=1}^{\lceil 3\rho \rceil} \frac{\exp(-e^{-2\rho/j})}{2\rho/j} \approx \frac{\lceil 3\rho \rceil!}{(2\rho)^{\lceil 3\rho \rceil}} \exp\left(-\int_0^{\lceil 3\rho \rceil} e^{-2\rho/t} dt\right) \\ &\approx \frac{\lceil 3\rho \rceil!}{(2\rho)^{\lceil 3\rho \rceil - 1}} \exp\{-\lceil 3\rho \rceil \exp(-2\rho/\lceil 3\rho \rceil) \\ &\quad + 2\rho \,\mathrm{Ei}(-2\rho/\lceil 3\rho \rceil) + e^{-2\rho}\}, \end{aligned} \tag{71}$$

where Ei denotes the exponential integral

$$\mathrm{Ei}(x) = \int_{-\infty}^{x} \frac{e^t}{t} dt, \quad x \neq 0.$$

The second product in Eq. (55) may be reduced as

$$\prod_{j=1}^{k} (\ell_j - \ell_{j-1}) = \prod_{j=0}^{k-1} \{c(j+1)^2 - cj^2\} = \left(\frac{c}{2}\right)^k \frac{(2k)!}{k!}. \tag{72}$$

Finally, the third product in Eq. (55) becomes

$$\begin{aligned}&\prod_{j=0}^{k-1} \left\{\left(1+\frac{j^2c}{2}\right)x_k\right\}^{\rho c(2j+1)} \\ &\quad = x_k^{\rho c} \prod_{j=1}^{k-1} \left(\frac{j^2 c x_k}{2}\right)^{\rho c(2j+1)} \left(1+\frac{2}{j^2 c}\right)^{\rho c(2j+1)} \\ &\quad \approx (k^2 e)^{2\rho} (2/c)^{\rho c} \exp\left(-\frac{2\rho}{x_k}\right)\left(\frac{(k!)^2}{k^{2(k+1)}}\right)^{\rho c}. \end{aligned} \tag{73}$$

Upon applying Stirling's formula $k! \approx \sqrt{2\pi} e^{-k} k^{k+0.5}$ and making the substitution $k^2 c/2 \approx 1/x_k$ for large k, we have

$$\begin{aligned}&\prod_{j=0}^{k-1} \left\{\left(1+\frac{j^2c}{2}\right)x\right\}^{\rho c(2j+1)} \\ &\quad \approx \left(\frac{4\pi}{c}\right)^{\rho c}\left(\frac{2e}{cx_k}\right)^{2\rho}\left(\frac{cx_k}{2}\right)^{\rho c/2} \\ &\quad \times \exp\left(-\frac{2\rho}{x_k} - 2\rho c\sqrt{\frac{2}{cx_k}}\right). \end{aligned} \tag{74}$$

Multiplying Eq. (70), Eq. (72), and Eq. (74), we have for the lower bound $\underline{G}_n(x_k)$

$$\begin{aligned}\underline{G}_n(x_k) = \mu_k(n) &= (n-2/x_k)\underline{\aleph}(c,\rho)\left(\frac{cx_k}{2}\right)^{(\rho/2)(c-4)+1/4} \\ &\quad \times \exp\left(-\underline{B}\frac{2\rho}{x_k}\right), \end{aligned} \tag{75}$$

where

$$\underline{\aleph}(c,\rho) = \Phi(\rho)\left(\frac{4\pi}{c}\right)^{\rho c}\frac{e^{2\rho}}{\sqrt{\pi}} \tag{76}$$

and

$$\underline{B} = 1 + \left[2c - \frac{\ln(4\rho c)}{\rho}\right]\sqrt{\frac{x_k}{2c}}. \tag{77}$$

A similar calculation may be carried out for the upper bound $\overline{G}_n(x_k)$. Manipulating the expression for $\mu_r(n)$ in Eq. (55) as before, we get

$$\begin{aligned}\overline{G}_n(x_k) = \mu(n) &= (n-2/x_k)\overline{\aleph}(c,\rho)\left(\frac{cx_k}{2}\right)^{(\rho/2)(c-4)+3/4} \\ &\quad \times \exp\left(-\overline{B}\frac{2\rho}{x_k}\right), \end{aligned} \tag{78}$$

where

$$\overline{\aleph}(c,\rho) = \Phi(\rho)\left(\frac{1}{2\pi}\right)^{\rho c}\frac{e^{-2\rho}}{\sqrt{\pi}}\frac{1}{2c} \tag{79}$$

and

$$\overline{B}=1-\left[2c+\frac{\ln(4\rho c)}{\rho}\right]\sqrt{\frac{x_k}{2c}}. \tag{80}$$

Equations (75) and (78) are the bounding probabilities of failure of a LLS composite bundle under applied load x_k. It is important to note that, while desirable, the bounds $\overline{G}_n(x_k)$ and $\underline{G}_n(x_k)$ are not asymptotically convergent as $x_k \downarrow 0$. In fact,

$$\frac{\overline{G}_n(x_k)}{\underline{G}_n(x_k)} \sim \sqrt{x_k}\exp\left(\sqrt{\frac{32\rho^2 c}{x_k}}\right), \tag{81}$$

which blows up as $x_k \downarrow 0$.

In applying the Chen-Stein theorem to obtain Eq. (19), and also elsewhere, we made the approximation that, for small λ, $\lambda \approx 1-\exp(-\lambda)$. Reversing this procedure presently, we may write

$$\underline{G}_n(x_k) \approx 1-\exp\left[-(n-2/x_k)\underline{\aleph}(c,\rho) \times\left(\frac{cx_k}{2}\right)^{(\rho/2)(c-4)+1/4}\exp\left(-\underline{B}\frac{2\rho}{x_k}\right)\right] \tag{82}$$

and

$$\overline{G}_n(x_k) \approx 1-\exp\left[-(n-2/x_k)\overline{\aleph}(c,\rho) \times\left(\frac{cx_k}{2}\right)^{(\rho/2)(c-4)+3/4}\exp\left(-\overline{B}\frac{2\rho}{x_k}\right)\right], \tag{83}$$

on the basis of Eqs. (75) and (78).

IV. DISCUSSION

Despite not obtaining converging tight bounds as k increases and x_k decreases, the above forms of $\overline{G}_n(x_k)$ and $\underline{G}_n(x_k)$ suggest the following form for the strength distribution of n-fiber bundles with power law distributed fibers. In writing it we drop the subscript in x_k, and permit x to vary continuously:

$$\tilde{G}_n(x)=1-\exp\left[-(n-2/x)\tilde{\aleph}(c,\rho)\left(\frac{cx}{2}\right)^{(\rho/2)(c-4)+\varphi_1} \times\exp\left(-\tilde{B}\frac{2\rho}{x}\right)\right], \tag{84}$$

where $\tilde{B}=1+[\varphi_2-\ln(4\rho c)/\rho]\sqrt{x/2c}$ with $-2c\leqslant\varphi_2\leqslant 2c$ and $1/4\leqslant\varphi_1\leqslant 3/4$. Also, $\tilde{\aleph}$ must be bounded between $\underline{\aleph}$ and $\overline{\aleph}$. If κ is the critical cluster size as defined below Eq. (8), then for $\kappa \gg 1$, $\kappa \approx 2/x$. Thus, the $(n-2/x)$ term in the above equation may be replaced with $n-\kappa$. In the practically interesting case of $n \gg \kappa$, this factor can simply be replaced by n. It is also worth mentioning that, if the calculations of the preceding sections had been carried out with circular, instead of open boundary conditions, the factor n would have occurred in place of $n-2/x=n-\kappa$ in the above equation.

Substituting Eq. (84) in Eq. (4), we obtain

$$\tilde{H}_{m,n}(x)\approx 1-\exp\left[-m(n-2/x)\tilde{\aleph}(c,\rho) \times\left(\frac{cx}{2}\right)^{(\rho/2)(c-4)+\varphi_1}\exp\left(-\tilde{B}\frac{2\rho}{x}\right)\right] \tag{85}$$

for the composite strength distribution. Note that mn here represents the volume of the composite. Equation (85) can thus be interpreted as giving a size scaling for the composite strength distribution.

Equation (84) is strikingly similar to that derived heuristically by Phoenix and Beyerlein [29] for the strength distribution function in the present problem. Phoenix and Beyerlein's formula is based on Smith's formula, but additionally accounts for the ''stalling'' of a κ cluster in Eq. (8), i.e., the event that the continued propagation of a κ cluster is blocked by particularly strong fibers at its ends. Since their failure event is a subset of Smith's, their strength distribution function is no greater than Smith's distribution function. For the n-fiber bundle subjected to load x per fiber, Phoenix and Beyerlein [29] obtain

$$\tilde{\tilde{G}}_n(x)=1-\exp\left[-n\tilde{\tilde{\aleph}}(\rho)\left(\frac{x}{2}\right)^{-3\rho/2}\exp\left(-\tilde{\tilde{B}}\frac{2\rho}{x}\right)\right], \tag{86}$$

where

$$\tilde{\tilde{B}}=2^{-1/\rho}\left[1+\frac{1}{\rho^2}\left(\Gamma(1/\rho,1)+\frac{\rho}{2(\rho+1)}\right)\right] \tag{87}$$

and $\Gamma(1/\rho, 1)$ refers to the incomplete gamma function. Also, for $\tilde{\tilde{\aleph}}$ they have

$$\tilde{\tilde{\aleph}}(\rho)=\frac{2^\rho e^{3\rho}}{2^{5/2}3^{5\rho/2}}. \tag{88}$$

Comparing Eq. (84) and Eq. (86), it is immediately seen that the exponential factors are almost the same since $\tilde{B} \approx \tilde{\tilde{B}} \approx 1$ in the lower tail, and the preexponential power factor would also be almost the same (except for φ_1) if $c=1$. We will now show that for $\rho \geqslant 1$ and taking $c=1$, while the bounding distributions $\underline{G}_n(x)$ and $\overline{G}_n(x)$ [Eqs. (75) and (78)] closely approximate Eq. (86), where it is successful in capturing the actual bundle strength distribution (as seen from simulations), the bounds [especially $\overline{G}_n(x)$] also succeed in $\rho<1$ with $c>1$ where Eq. (86) breaks down.

The question thus arises as to the choice of c. Clearly, choosing $c=1$ in Eq. (60) and Eq. (61) will result in the finest possible discretization, which nevertheless is coarser than the true fiber strength distribution. However, choosing $c=1$ regardless of the value of ρ may result in loose error bounds [which vary as $O(1/c)$] in Eq. (56). Thus c should be chosen large enough that the errors in Eq. (56) are small, while not so large that it is an overly coarse discretization of the given power law distribution. When the fiber strengths are power law distributed, it can be seen from Eq. (18) even

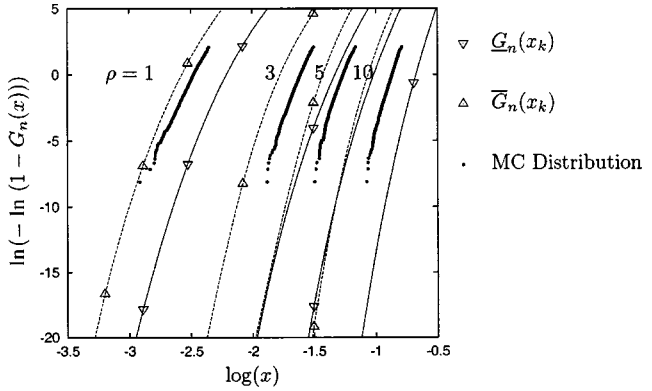

FIG. 4. Comparison of Monte Carlo (MC) generated empirical strength distributions with the upper and lower bounds on the strength distribution when $\rho \geqslant 1$. The upper and lower bounds are calculated only at the points [$x = x_k$, Eq. (59)] shown; the lines are *C*-spline interpolations between these points, intended merely to guide the eye. For all these ρ, it suffices to assume that $c = 1$, as seen in Table I.

in the simplest case of a 0-1 bundle that c must increase as ρ decreases in order to keep the error bound $(2\alpha\lambda_1)/(\ell_1\beta_1)$ constant for fixed λ_1.

To determine the value of c, empirical strength distributions of bundles of $n = 2^{20}$ fibers were generated from 2^{11} Monte Carlo replications of bundle failure under idealized local load sharing. The simulation algorithm is the static version of Newman and Phoenix's [27] time-dependent simulation algorithm. We used this algorithm to calculate the empirical distribution down to $\rho = 1/128$. For smaller ρ than this, numerical round-off errors seem to become a problem. In fact, the upper tail of the calculated empirical distribution for $\rho = 1/128$ is not reliable for this reason. Figures 4 and 5 show the empirical strength distributions on Weibull probability paper for a range of ρ, the power law exponent, which inversely governs the fiber strength variability. Also shown are the upper and lower bounds $\overline{G}_n$ and $\underline{G}_n$. Within the probability range of the simulations, especially for larger ρ, k given by Eq. (59) is so small that the approximations made to obtain the asymptotic formulas Eq. (75) and Eq. (78) become inaccurate. Therefore the bounds plotted in these figures are obtained by evaluating the products directly; for example, the lower bound plotted in these figures is obtained by evaluating the products on the left hand side of Eq. (70), Eq. (72), and Eq. (74), at each $x = x_k$ given by Eq. (59). [Recall from Eq. (59) that the corresponding critical cluster size is given by $k^2 c$.] The figures also show curves connecting the calculated distribution function values at different $x = x_k$. These smooth curves are obtained by numerical interpolation with *C* splines.

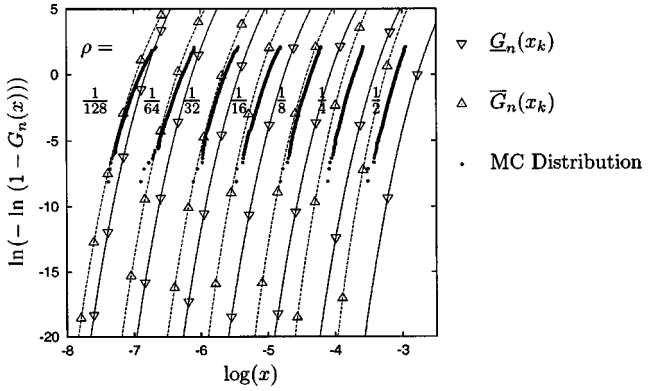

FIG. 5. Comparison of Monte Carlo (MC) generated empirical strength distributions with the upper and lower bounds on the strength distribution for $0 < \rho < 1$. The upper and lower bounds are calculated only at the points [$x = x_k$, Eq. (59)] shown; the lines are *C*-spline interpolations between these points. Note that $c > 1$ and c increases with decreasing ρ as seen in Table I.

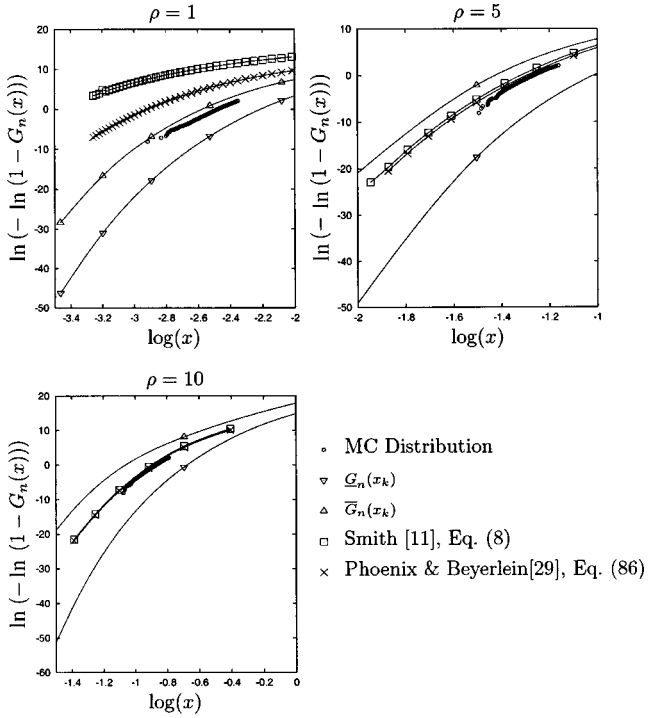

FIG. 6. Comparison of Monte Carlo (MC) generated empirical bundle strength distribution with Smith's formula, Phoenix and Beyerlein's formula, and the presently calculated upper and lower bound formulas $\overline{G}_n$, and $\underline{G}_n$ (assuming $c = 1$) for $\rho = 1$, $\rho = 5$, and $\rho = 10$.

Figure 6 shows the predictions of Smith's formula, Phoenix and Beyerlein's model, and the presently calculated upper and lower bound formulas $\overline{G}_n$ and $\underline{G}_n$, together with Monte Carlo simulation generated empirical strength distributions on the same plot, for each of $\rho = 1$, 5, and 10, for comparison. As in Figs. 4 and 5, the bounding distributions are calculated only at $x = x_k$, given by Eq. (59) but interpolated using *C* splines. Also, the abscissa x_κ for each point in the curve plotting Smith's formula corresponds to an integral κ according to $(1 + \kappa/2)x_\kappa = 1$. (Note that we distinguish between Smith's abscissas x_κ and our x_k's.) As is clearly seen, the Smith and the Phoenix and Beyerlein formulas coincide for $\rho = 10$. However, a small divergence is already seen at $\rho = 5$, which widens at $\rho = 1$. As stated earlier, the Phoenix and Beyerlein $\tilde{\overline{G}}_n$ of Eq. (86) is less than that of Smith's formula owing to its stricter definition of composite failure.

Also, in comparing with the empirical strength distribution obtained from Monte Carlo simulations, we find that Phoenix and Beyerlein's formula generally deteriorates as an approximation of the empirical distribution with decreasing ρ. The calculated $\bar{G}_n$ and G_n, however, continue to bound the empirical distributions even at small ρ, and, in fact, it appears that the upper bound $\bar{G}_n$ becomes an increasingly good approximation of the empirical distribution as ρ decreases.

We now consider how Smith's formula should be modified so as to succeed in fitting the empirical strength distribution at low ρ as well. Comparing Smith's formula Eq. (8) with the components of $G_n(x)$, we first observe from Eq. (74) that it approximately corresponds to the product $K_1^\rho K_2^\rho \cdots K_{\kappa-1}^\rho x^{\kappa\rho}$ in Eq. (8). Thus the essential difference between Eq. (8) and $G_n(x)$ given by Eq. (75) is that the product of Eq. (70) and Eq. (72) replaces the factor 2^κ in Eq. (8). This product is

$$[\text{Eq. (70)}\times\text{Eq. (72)}] \approx \Phi(\rho)\frac{(2\rho)^k}{k!}\left(\frac{c}{2}\right)^k\frac{(2k)!}{k!}$$

$$\approx \Phi(\rho)\frac{(4\rho c)^k}{\sqrt{\pi k}}$$

$$\approx \Phi(\rho)\left(\frac{cx_k}{2}\right)^{1/4}(4c\rho)^{\sqrt{2/cx_k}}. \qquad (89)$$

The important point here is that the factor 2^κ in Smith's formula is replaced by a factor that varies as $\Phi(\rho)(4\rho c)^k/\sqrt{\pi k}$. To compare with Smith's prefactor of 2^κ, we observe that Smith's critical cluster size is κ, while the present calculation's critical cluster size is k^2c, for a fixed stress level. Equating these two, we find that the correct prefactor in Smith's formula should be

$$[\Phi(\rho)\sqrt[4]{c}/\sqrt{\pi}]f^{\sqrt{\kappa}}/\sqrt[4]{\kappa}, \quad f=(4\rho c)^{1/\sqrt{c}}. \qquad (90)$$

In this, $f^{\sqrt{\kappa}}/\sqrt[4]{\kappa}$ represents the part that varies with κ.

Figure 7 plots the variation of this prefactor for a range of κ. In calculating f for different ρ, the values of c from Table I have been assumed. The figure also shows a line corresponding to Smith's prefactor of 2^κ. Scaling Eq. (90) (i.e., sliding the curves down vertically in Fig. 7) for $\rho=3$, 5, and 10 will bring the prefactor of Eq. (90) into approximate agreement with Smith's 2^κ curve in the small κ regime of the present Monte Carlo simulations. [The lowest stress level attained in the $\rho=5$ simulation of Fig. 6, $\ln(x)\approx-1.5$, corresponds approximately to $\kappa=7$.] For larger κ corresponding to the deep lower tail beyond the reach of present simulations, Fig. 7 suggests the breakdown of Smith's and Phoenix and Beyerlein's formulas even for large ρ. At small ρ, where even within the regime of the simulations the critical cluster size κ is large, Fig. 7 clearly demonstrates the reason for the breakdown of the heuristic formulas: A pronounced gap between Smith's 2^κ curve, and that obtained from Eq. (90). At $\rho=1/128$, the prefactor actually decreases slowly with increasing κ, unlike 2^κ.

The conclusions above are also true for the upper bound, where the corresponding factor in terms of applied stress is

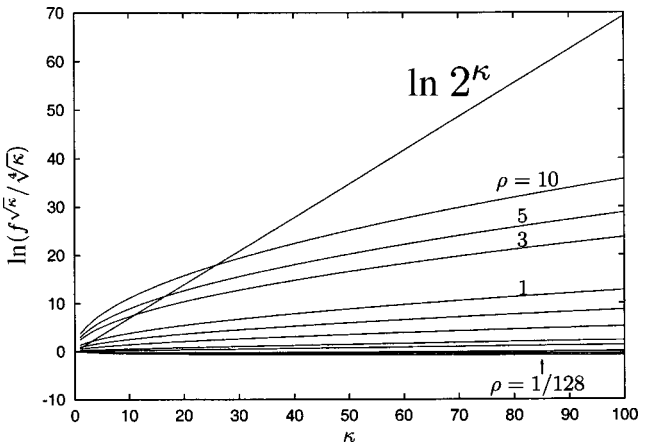

FIG. 7. Variation of the prefactor Eq. (90) with κ for different values of ρ. The unmarked curves below $\rho=1$ correspond to $\rho=1/2$, 1/4, 1/8, 1/16, 1/32, and 1/64 as one moves downward. Also shown here is a line for Smith's prefactor of 2^κ. The rate of increase of the prefactor from Eq. (90) is clearly slower than that of Smith's, for all ρ.

$$\frac{\Phi(\rho)}{2c\sqrt{\pi}}\left(\frac{cx_k}{2}\right)^{3/4}(4c\rho)^{\sqrt{2/cx_k}}. \qquad (91)$$

It was noted in Sec. I that Smith's model assumes that the two fibers adjacent to a κ cluster are fresh, and the failure probability of at least one of them is approximately $2F(K_\kappa x)$. However, the fibers may have seen some prior load which would decrease their conditional probability of failure [Eq. (9)], especially for smaller ρ. This correction was also noted as being excessive. In view of the above discussion, it may therefore be inferred that the product of the corrections must have the form given by Eq. (90).

V. CONCLUSIONS

By using the Chen-Stein theorem for Poisson approximations, we have bounded the strength distribution of a planar LLS composite bundle [and composite, using Eq. (4)] with fibers whose strengths are distributed according to a power law distribution $F(x)=x^\rho 1_{[0\le x\le 1]}+1_{[x>1]}$. The bounds, especially the upper one, seem to be reasonably good ap-

TABLE I. Variation of the parameter c with ρ as determined by Monte Carlo simulations of large bundle failure.

ρ	$c(\rho)$	ρ	$c(\rho)$	ρ	$c(\rho)$
$\frac{1}{128}$	40	$\frac{1}{8}$	4	3	1
$\frac{1}{64}$	23	$\frac{1}{4}$	3	5	1
$\frac{1}{32}$	12	$\frac{1}{2}$	2	10	1
$\frac{1}{16}$	8	1	1		

proximations of the actual composite distribution for all ρ as seen in comparisons with Monte Carlo simulations. The fact that such bounding is possible also shows that the composite failure mode is brittle for all ρ. The closed form expressions for the bounds also allow us to see what was unknown before: Smith's formula Eq. (8) can predict the strength distribution for all ρ if its prefactor 2^{κ} is corrected to Eq. (90).

The next questions of obvious interest are those of whether these results apply to other, similar model materials, and if so, to what extent? While it would be incautious to speculate on answers, for experience shows that the strength of a random heterogeneous material depends subtly and sensitively on the details of its microscopic flaw strengths and micro-mechanical load redistribution, we will now briefly describe some of the questions.

The power law probability measure assumed in this work has a compact support on [0,1]. More realistic probability distributions for fiber strength, such as the Weibull distribution Eq. (5), may, however, have a heavy upper tail when ρ is small (although the realism of this is certainly open to question since the fiber strength is ultimately bounded by the atomic bond strength). Qualitatively, a heavy upper tail implies a sizable probability that a growing cluster of fiber breaks will encounter a particularly strong fiber which may block its advance. Whether such hindrance to cluster growth will impact the overall statistics of composite strength in the lower tail and give it a tough character for $\rho<\rho_{\mathrm{th}}$, where ρ_{th} is some threshold, is unknown, especially for realistic bundle sizes far beyond current numerical simulation capability.

While the above pertains to fiber strength randomness, the concern of the following questions lies in the load sharing in partially damaged composite bundles. We must first note that LLS in a planar composite bundle is a severely localized form of load sharing, which best encourages the extension of a crack (cluster of breaks) by failing strength elements (fibers) surrounding it. That is, it encourages brittle fracture. In reality, load sharing is more long range. While the greatest stress concentration around a cluster of breaks still occurs on the neighbors of a cluster, fibers further away also typically carry some overload. To describe this situation parametrically, we may think of overload decay away from a fiber break as occurring according to

$$K_{\iota}=K_0/\iota^{\nu}, \tag{92}$$

where K_0 is the stress concentration on the two intact neighbors of a broken fiber, $\iota=1$ indexes the two fibers adjacent to a single fiber break, $\iota=2$ the two subadjacent fibers and so on. It is easy to see that $\nu=\infty$ corresponds to LLS, while $\nu=0$ corresponds to ELS described in Sec. I. Also, the load sharing scheme due to Hedgepeth, realistic for an elastic bonded fiber and matrix, corresponds to $\nu=2$. Knowing that $\nu=0$ (ELS) corresponds to a tough failure mode (Daniels [1]) and $\nu=\infty$ (LLS) to a brittle mode, a natural question is the following: Is there a sharp boundary in the ρ-ν plane that separates it into a brittle regime and a tough regime? If so, its location would be interesting from both theoretical and practical standpoints.

The lessening of the stress concentration ahead of a break which may lead to an overall tough failure mode can also occur for other reasons. In a three-dimensional LLS bundle (Smith *et al.* [30]), a greater number of fibers surround a broken fiber than in a two-dimensional bundle. This lowers the probability that an intact fiber ahead of a break will break and qualitatively could result in an overall tough failure mode at least for some range of ρ. Similarly if, unlike in the present model, fiber breaks were allowed to be staggered along the length of a bundle, the stress concentration caused by a cluster of breaks would be lowered below that caused by a cluster of transversely aligned breaks. It is not known if this impels the overall statistics toward the tough failure regime.

In view of these and many other unresolved questions about the fracture behavior of a composite, a prototypical random heterogeneous material, it can be safely stated that there is a long way to go before one can claim a reasonably comprehensive understanding of the extreme value dependence between the microscopic fracture processes and bulk fracture. Piecing together such understanding will require blending together physical reasoning, probabilistic methodology, computational techniques, and experiments. Relying exclusively on computer simulations of small systems ($<10^4$ fibers) is likely to result in inconclusive, or worse, incorrect understanding of the complex strength statistics of these material systems.

ACKNOWLEDGMENTS

S.L.P. acknowledges support from the Institute for Future Space Transport funded under a NASA URETI grant and monitored through NASA Glenn Research Center. S.M. acknowledges support from the DOE, Office of Science, Office of Basic Energy Sciences.

APPENDIX A: THE CHEN-STEIN METHOD

As described by Arratia *et al.* [31], the Chen-Stein method of Poisson approximation is a powerful tool for computing an error bound when approximating probabilities using the Poisson approximation. Let I be an arbitrary index set and suppose $\{Y_i, i\in I\}$ are 0–1 Bernoulli random variables with $p_i=\mathrm{Prob}\{Y_i=1\}>0$. Then $p_i=\mathbf{E}[Y_i]$ and we let

$$\lambda=\sum_{i\in I} p_i \quad \text{and} \quad T=\sum_{i\in I} Y_i. \tag{A1}$$

Also let W be a Poisson random variable with mean $\lambda\in(0,\infty)$. For each $i\in I$ let J_i denote an arbitrarily chosen set of *near neighbors* of i and let

$$V_i=T-\sum_{j\in J_i} Y_j. \tag{A2}$$

We think of J_i as the neighborhood of dependence of i such that Y_i is independent or nearly independent of Y_j for $j\notin J_i$. Then for $A\subseteq\mathbb{Z}_+$ the Chen-Stein theorem asserts that

$$
\begin{aligned}
&|\mathrm{Prob}\{T\in A\}-\mathrm{Prob}\{W\in A\}| \\
&\leqslant \Delta f \sum_{i\in I}\sum_{j\in J_i} p_i p_j + \Delta f \sum_{i\in I}\sum_{j\in J_i}\mathbf{E}[Y_i Y_j] \\
&\quad + \left|\sum_{i\in I}\mathbf{E}\{(Y_i-p_i)f(V_i+1)\}\right| \\
&= b_1+b_2+b_3, \qquad \text{(A3)}
\end{aligned}
$$

where f is a function for which $\|f\|\leqslant\min(1,1.4\lambda^{-1/2})$ and $\Delta f\leqslant\min(1,1/\lambda)$. The b_1,b_2,b_3 notation was given by Arratia *et al.* [31]. Loosely, b_1 measures the neighborhood size, b_2 the expected number of neighboring occurrences of a given occurrence, and b_3 the dependence between an event and the number of occurrences outside its neighborhood of dependence.

APPENDIX B: DOMINATED CONFIGURATIONS OF A 0-1-2 BUNDLE

It will be shown here that all other configurations listed in Sec. II C 1 have probability whose order of magnitude is smaller than Prob{Eq. (23)∪Eq. (26)}. We begin with the configurations Eq. (21) and Eq. (22). Their union starting at fiber i is a subset of the event

$$
\begin{array}{c}
i \qquad\qquad\qquad \downarrow \\
2_1\ \underbrace{0\ \cdots\ 0}_{0\leq s<\ell_2}\ 2\ \underbrace{0\ \cdots\ 0}_{\ell_2-s}
\end{array}
\qquad \text{(B1)}
$$

so that

$$
\begin{aligned}
&\mathrm{Prob}\{\text{Eq. (21)}\cup\text{Eq. (22)}\} \\
&\quad\leqslant \mathrm{Prob}\{\text{Eq. (B1)}\} \\
&\quad= \mathrm{Prob}\{\text{Eq. (23)}\cup\text{Eq. (26)}\}O(\gamma_1^L). \qquad \text{(B2)}
\end{aligned}
$$

Next consider the superset of events Eq. (24) and Eq. (25):

$$
\begin{array}{c}
i \qquad\qquad\qquad\qquad \downarrow \\
2_1\ \underbrace{0\ \cdots\ 0}_{L\leq s<\ell_2-(\ell_1+1)}\ 2\ \underbrace{1_0\ \cdots\ 1_0\ \langle 0\text{-}1\rangle\ 1_0\ \cdots\ 1_0}_{\ell_2-s}.
\end{array}
\qquad \text{(B3)}
$$

Here we have

$$
\begin{aligned}
&\mathrm{Prob}\{\text{Eq. (24)}\cup\text{Eq. (25)}\} \\
&\quad\leqslant \beta_2(\beta_1+\beta_2)(\alpha+\beta_1+\beta_2)^{n_2-(\ell_2+2)} \\
&\qquad\times \sum_{s=L}^{\ell_2-(\ell_1+2)} \alpha^s \mu_1(\ell_2-s) \\
&\quad= \mathrm{Prob}\{\text{Eq. (23)}\cup\text{Eq. (26)}\}O(\gamma_1^L). \qquad \text{(B4)}
\end{aligned}
$$

By a similar calculation, it may be seen that the probability of Eq. (27) is also Prob{Eq. (23)∪Eq. (26)}$O(\gamma_1^L)$. Next for Eq. (28) we have

$$
\begin{aligned}
\mathrm{Prob}\{\text{Eq. (28)}\} &= \beta_2^2(\alpha+\beta_1+\beta_2)^{n_2-(\ell_2+2)} \sum_{s=\ell_1+2}^{\ell_2-(\ell_1+2)} \mu_1(s)\mu_1(\ell_2-s) \\
&\leqslant \frac{\beta_2^2 C_0}{6(\alpha+\beta_1+\beta_2)^2}(\alpha+\beta_1+\beta_2)^{n_2-\ell_2}\mu_1(\ell_2)\left(\frac{\ell_1[(\ell_2-2\ell_1)\vee 0]^3}{\ell_2-\ell_1}\gamma_1^{\ell_1}\right) \\
&= \mathrm{Prob}\{\text{Eq. (23)}\cup\text{Eq. (26)}\}O\left(\frac{\ell_1[(\ell_2-2\ell_1)\vee 0]^3}{\ell_2-\ell_1}\gamma_1^{\ell_1}\right). \qquad \text{(B5)}
\end{aligned}
$$

Note here that if

$$
\frac{\ell_1(\ell_2-2\ell_1)^3}{\ell_2-\ell_1}\gamma_1^L=\Omega(1)
$$

the contribution of Prob{Eq. (28)} will be quite substantial in comparison to Prob{Eq. (23)∪Eq. (26)}. Next,

$$
\begin{aligned}
\mathrm{Prob}\{\text{Eq. (29)}\} &\leqslant \beta_2(C_0\ell_1\alpha^{\ell_1})(\alpha+\beta_1)^{\ell_2-\ell_1} \sum_{s=0\vee(\ell_2-2\ell_1)}^{\ell_2-(\ell_1+3)} \alpha^{\ell_2-\ell_1-s-1}(\alpha+\beta_1+\beta_2)^{n_2-(\ell_2+1)-(\ell_2-\ell_1-s-1)} \\
&\leqslant \frac{\beta_2\alpha^2}{(\beta_1+\beta_2)(\alpha+\beta_1+\beta_2)^2}(\alpha+\beta_1+\beta_2)^{n_2-\ell_2}\frac{\mu_1(\ell_2)}{\ell_2-\ell_1} \\
&= \mathrm{Prob}\{\text{Eq. (23)}\cup\text{Eq. (26)}\}O\left(\frac{1}{\ell_2-\ell_1}\right)
\end{aligned}
$$

and

$$\begin{aligned}\text{Prob}\{\text{Eq. (30)}\} &\leq \beta_2(\ell_1\beta_1^2\alpha^{\ell_1})(\alpha+\beta_1+\beta_2)^{n_2-(\ell_2+1)} \\ &\quad\times\sum_{s=\ell_2-(\ell_1+2)}^{\ell_2-1}(\alpha+\beta_1)^s \\ &\leq \frac{\beta_2(\alpha+\beta_1+\beta_2)}{1-(\alpha+\beta_1)}(\alpha+\beta_1 \\ &\quad+\beta_2)^{n_2-(\ell_2+2)}\frac{\mu_1(\ell_2)}{\ell_2-\ell_1} \\ &= \text{Prob}\{\text{Eq. (23)}\cup\text{Eq. (26)}\} \\ &\quad\times O(1/(\ell_2-\ell_1)).\end{aligned}$$

Finally, we have

$$\begin{aligned}\text{Prob}\{\text{Eq. (31)}\} &\leq (\ell_1\alpha_1^{\ell_1}\beta_1^2)(\alpha+\beta_1)^{\ell_2} \\ &= \text{Prob}\{\text{Eq. (23)}\cup\text{Eq. (26)}\} \\ &\quad\times O\left(\frac{(\alpha+\beta_1)^{\ell_1}}{\ell_2-\ell_1}\right).\end{aligned} \tag{B6}$$

Adding all these probabilities, we have for $p+L\leq i<p+n_2-\ell_2-1$

$$\begin{aligned}\text{Prob}\{Y_i=1\} &= \frac{\beta_2(\alpha+\beta_1)(2\alpha+\beta_1)(\beta_1+\beta_2)^2}{\beta_1(\alpha+\beta_1+\beta_2)^2\{(\alpha+\beta_1)(\beta_1+\beta_2)+\alpha\beta_1\}} \\ &\quad\times\mu_1(\ell_2)(\alpha+\beta_1+\beta_2)^{n_2-\ell_2} \\ &\quad\times\left\{1\pm O\left(\gamma_1^L+\frac{\ell_1\{(\ell_2-2\ell_1)\vee 0\}^3}{\ell_2-\ell_1}\gamma_1^{\ell_1}\right)\right\}.\end{aligned} \tag{B7}$$

As in the 0-1 case, we turn our attention next to the failure configurations that start very close to the boundary of the 0-1-2 subcomposite. That is, we consider i such that $p\leq i<p+L$ and evaluate the probabilities of the configurations listed in Sec. II C 1. Equation (32) continues to hold for Prob{Eq. (23)}. However, the event Eq. (26) may be decomposed according to whether $i\leq s$ or not:

$$\begin{array}{l} i \qquad\qquad\qquad\qquad\qquad\qquad \downarrow \\ 2\underbrace{1_0\ \cdots\ 1_0\ \langle 0\text{-}1\rangle\ 1_0\ \cdots\ 1_0}_{\ell_2-s}\,2\underbrace{0\ \cdots\ 0}_{i\leq s<L}\ \text{if } i\leq s\,. \end{array} \tag{B8}$$

If $i>s$, the configuration remains Eq. (26) with s constrained to lie in the range $1\leq s<i$. Prob{Eq. (26)} is now given by

$$\begin{aligned}\text{Prob}\{\text{Eq. (26)}\} &= (\beta_1+\beta_2)\beta_2^2 \\ &\quad\times\sum_{s=i-p+1}^{L-1}\sum_{t=0}^{s-1}\alpha^{s+t}\mu_1(\ell_2-s) \\ &\quad\times(\alpha+\beta_1+\beta_2)^{n_2-(\ell_2+t+3)} \\ &\quad+\beta_2^2\sum_{s=1}^{i-p}\alpha^s\mu_1(\ell_2-s) \\ &\quad\times(\alpha+\beta_1+\beta_2)^{n_2-(\ell_2+2)}.\end{aligned} \tag{B9}$$

The first term in Eq. (B9) reduces to Eq. (33). The second term when simplified becomes

$$\begin{aligned}&\frac{\alpha^2\beta_2^2}{(\alpha+\beta_1)(\beta_1+\beta_2)+\alpha\beta_1}\mu_1(\ell_2)(\alpha+\beta_1+\beta_2)^{n_2-(\ell_2+2)} \\ &\quad\times[1-(\gamma_1\gamma_2)^{i-p+1}]\left\{1\pm O\left(\frac{1}{\ell_1}+\frac{1}{\ell_2-\ell_1}\right)\right\}.\end{aligned} \tag{B10}$$

That the probability of all the other configurations is dominated by Prob{Eq. (23)$\cup$Eq. (26)} may be seen in the same way as before.

Next consider the case $i=p-1$. Then

$$\text{Prob}\{\text{Eq. (23)}\} = \frac{(\alpha+\beta_1)\beta_2}{\beta_1}\mu_1(\ell_2)(\alpha+\beta_1+\beta_2)^{n_2-(\ell_2+1)} \tag{B11}$$

and

$$\text{Prob}\{\text{Eq. (26)}\} = \frac{\alpha\beta_2}{\beta_1}\mu_1(\ell_2)(\alpha+\beta_1+\beta_2)^{n_2-(\ell_2+1)}. \tag{B12}$$

APPENDIX C: POISSON APPROXIMATION ERROR FOR A 0-1-2 BUNDLE

We now bound the Chen-Stein error $b_1+b_2+b_3$ arising from the Poisson approximation of the dependent process Y_i. We begin by defining $J_i=\{j:|j-i|\leq\ell_2+L+1\}$ so that random variables Y_i and $\{Y_j:j\notin J_i\}$ are independent and, consequently, $b_3=0$. As before,

$$\begin{aligned}b_1 &\leq \min(1,1/\lambda_2)2(n_2-\ell_2-1)(\ell_2+L+1) \\ &\quad\times[\lambda_2/(n_2-\ell_2-1)]^2 \\ &= \min(1,1/\lambda_2)2(\ell_2+L+1)\lambda_2^2/(n_2-\ell_2-1).\end{aligned} \tag{C1}$$

Bounding b_2 requires finding pairs of failure configurations such that $Y_iY_j=1, j\in J_i$. If one or both of Y_i and Y_j arise from a configuration different from Eq. (23) and Eq. (26), we know that the probability of the resulting overlapped configuration is Prob{Eq. (23)$\cup$Eq. (26)}$O(\ell_1^{-1}+(\ell_2-\ell_1)^{-1})$. Therefore we need consider only overlaps of Eq. (23) and Eq. (26).

Configurations of the form Eq. (23) may overlap themselves to produce $Y_iY_j=1$, for $j\in J_i$ as

$$\begin{array}{l} \overset{i}{2_1}\; \underbrace{0\cdots 0}_{0\le s_1<L}\; \overset{\downarrow}{2}\; \underbrace{1_0\cdots 1_0\,\langle 0\text{-}1\rangle\, 1_0\cdots 1_0}_{\ell_2-s_1-w-1}\; \overset{j}{1}\; \underbrace{0\cdots 0}_{w\le s_2<L}\ldots \\ \qquad\qquad\qquad\qquad\quad\; \ldots\, \overset{\downarrow}{2}\; \underbrace{1_0\cdots 1_0\,\langle 0\text{-}1\rangle\, 1_0\cdots 1_0}_{\ell_2-s_2} \end{array} \tag{C2}$$

and

$$\begin{array}{l} \overset{i}{2_1}\; \underbrace{0\cdots 0}_{0\le s_1<L}\; \overset{\downarrow}{2}\; \underbrace{1_0\cdots 1_0\,\langle 0\text{-}1\rangle\, 1_0\cdots 1_0}_{\ell_2-s_1}\; \underbrace{2_0\cdots 2_0}_{0\le w<L-1}\; \overset{j}{2_1}\ldots \\ \qquad\qquad \ldots\, \underbrace{0\;\ldots\;0}_{0\le s_2<L}\; \overset{\downarrow}{2}\; \underbrace{1_0\cdots 1_0\,\langle 0\text{-}1\rangle\, 1_0\cdots 1_0}_{\ell_2-s_2}, \end{array} \tag{C3}$$

or they may overlap configurations Eq. (26) as

$$\begin{array}{l} \overset{i}{2_1}\; \underbrace{0\cdots 0}_{0\le s_1<L}\; \overset{\downarrow}{2}\; \underbrace{1_0\cdots 1_0\,\langle 0\text{-}1\rangle\, 1_0\cdots 1_0}_{\ell_2-s_1-w-1}\; 1\; \underbrace{0\cdots 0}_{w\le t<s_2}\ldots \\ \qquad\quad \ldots\, \overset{j}{2}\; \underbrace{1_0\cdots 1_0\,\langle 0\text{-}1\rangle\, 1_0\cdots 1_0}_{\ell_2-s_2}\; \overset{\downarrow}{2}\; \underbrace{0\;\ldots\;0}_{0\le s_2<L} \end{array} \tag{C4}$$

and

$$\begin{array}{l} \overset{i}{2_1}\; \underbrace{0\cdots 0}_{0\le s_1<L}\; \overset{\downarrow}{2}\; \underbrace{1_0\cdots 1_0\,\langle 0\text{-}1\rangle\, 1_0\cdots 1_0}_{\ell_2-s_1}\; \underbrace{2_0\cdots 2_0}_{0\le w<L-1}\ldots \\ \qquad\quad \ldots\, \overset{j}{2}\; \underbrace{1_0\cdots 1_0\,\langle 0\text{-}1\rangle\, 1_0\cdots 1_0}_{\ell_2-s_2}\; \overset{\downarrow}{2}\; \underbrace{0\;\ldots\;0}_{0\le s_2<L}. \end{array} \tag{C5}$$

Turning next to configurations in which Eq. (26) overlaps itself, we have $Y_iY_j=1, j\in J_i$, when

$$\begin{array}{l} 2_1\; \underbrace{0\cdots 0}_{0\le t<s_1}\; \overset{i}{2}\; \underbrace{1_0\cdots 1_0\,\langle 0\text{-}1\rangle\, 1_0\cdots 1_0}_{\ell_2-s_1}\; \overset{\downarrow\, j}{2}\; \underbrace{0\cdots 0}_{1\le s_1<L}\ldots \\ \ldots\; \underbrace{0\cdots 0}_{0\le s_2-s_1<L-s_1}\; \overset{\downarrow}{2}\; \underbrace{1_0\cdots 1_0\,\langle 0\text{-}1\rangle\, 1_0\cdots 1_0}_{\ell_2-s_2}\; 2\; \underbrace{0\;\ldots\;0}_{0\le s_2<L} \end{array} \tag{C6}$$

and

$$
\begin{array}{c}
\qquad\qquad\qquad\qquad i \qquad\qquad\qquad\qquad\qquad\qquad \downarrow j \\
2_1 \underbrace{0 \cdots 0}_{0\le t<s_1} 2 \underbrace{1_0 \cdots 1_0 \langle 0\text{-}1\rangle 1_0 \cdots 1_0}_{\ell_2-s_1} 2 \underbrace{0 \cdots 0}_{1\le s_1<L} \cdots \\
\qquad\qquad\qquad\qquad\qquad \downarrow \\
\cdots \underbrace{2_0 \cdots 2_0\, 2_1\, 0 \ldots 0}_{0\le w<s_2} 2 \underbrace{1_0 \cdots 1_0 \langle 0\text{-}1\rangle 1_0 \cdots 1_0}_{\ell_2-s_2} 2 \underbrace{0 \ldots 0}_{0\le s_2<L},
\end{array}
\tag{C7}
$$

and finally for configurations in which Eq. (26) overlaps Eq. (23) to produce $Y_i Y_j = 1, j \in J_i$, we have

$$
\begin{array}{c}
\qquad\qquad\qquad\qquad i \qquad\qquad\qquad\qquad\qquad\qquad \downarrow \\
2_1 \underbrace{0 \cdots 0}_{0\le t<s_1} 2 \underbrace{1_0 \cdots 1_0 \langle 0\text{-}1\rangle 1_0 \cdots 1_0}_{\ell_2-s_1} 2 \underbrace{0 \cdots 0}_{1\le s_1<L} \cdots \\
\qquad\qquad\qquad\quad j \qquad\qquad \downarrow \\
\cdots \underbrace{2_0 \cdots 2_0}_{0\le w<L} 2_1 \underbrace{0 \ldots 0}_{0\le s_2<L} 2 \underbrace{1_0 \cdots 1_0 \langle 0\text{-}1\rangle 1_0 \cdots 1_0}_{\ell_2-s_2}.
\end{array}
\tag{C8}
$$

In bounding the probability of these configurations the configuration

$$
2 \underbrace{1_0 \cdots 1_0 \langle 0\text{-}1\rangle 1_0 \cdots 1_0}_{\ell_2-L+1\le \ell_2-s_2<\ell_2}
\tag{C9}
$$

arises repeatedly and has probability

$$
\text{Prob}\{\text{Eq. (C9)}\} \le \beta_2 \sum_{s_2=0}^{L-1} (\alpha+\beta_1)^{\ell_2-s_2-(\ell_1+2)} (\ell_2-s_2-\ell_1-1) = \lambda_2 O\left(\frac{1}{(\alpha+\beta_1)^L}\right).
\tag{C10}
$$

With this result in hand, it is readily seen that Prob{Eq. (C2)} $=\lambda_2^2 O((\alpha+\beta_1)^{-L})$ since the probability of the fiber arrangement to the left of the second pressured element 2 is bounded from above by λ_2, the arrangement to the right of the second pressured element has probability bounded from above by $\lambda_2 O((\alpha+\beta_1)^{-L})$, and these two events are independent.

Similar arguments for the other configurations establish that the Poisson approximation error is $\lambda_2 O(\lambda_2/(\alpha+\beta_1)^L)$. Since $\lambda_2 = o(\alpha^L)$, the Poisson error is bounded more loosely by $\lambda_2 O(\alpha^L/(\alpha+\beta_1)^L) = \lambda_2 O(\gamma_1^L)$.

[1] H. E. Daniels, Proc. R. Soc. London, Ser. A **183**, 405 (1945).
[2] D.E. Gücer and J. Gurland, J. Mech. Phys. Solids **10**, 365 (1962).
[3] B. W. Rosen, AIAA J. **2**, 1985 (1964).
[4] P. M. Scop and A. S. Argon, J. Compos. Mater. **1**, 92 (1967).
[5] D. G. Harlow and S. L. Phoenix, J. Compos. Mater. **1**, 314 (1978).
[6] J. M. Hedgepeth, NASA Technical Report No. TND-882, 1961 (unpublished).
[7] W. Weibull, J. Appl. Mech. **18**, 293 (1951).
[8] S. Zhang and E. Ding, Phys. Rev. B **53**, 646 (1996).
[9] B. Q. Wu and P. L. Leath, Phys. Rev. B **59**, 4002 (1999).
[10] D. G. Harlow and S. L. Phoenix, Int. J. Fract. **15**, 331 (1979).
[11] R. L. Smith, Proc. R. Soc. London, Ser. A **373**, 539 (1980).
[12] C.-C. Kuo and S. L. Phoenix, J. Appl. Probab. **24**, 137 (1987).
[13] D. G. Harlow, Proc. R. Soc. London, Ser. A **397**, 211 (1985).
[14] P. M. Duxbury and P. L. Leath, Phys. Rev. B **49**, 12 676 (1994).
[15] D. G. Harlow and S. L. Phoenix, J. Mech. Phys. Solids **39**, 173 (1991).
[16] S. L. Phoenix and I. J. Beyerlein, Phys. Rev. E **62**, 1622 (2000).
[17] I. J. Beyerlein and S. L. Phoenix, Eng. Fract. Mech. **57**, 267 (1997).
[18] C. M. Landis, I. J. Beyerlein, and R. M. McMeeking, J. Mech. Phys. Solids **48**, 621 (2000).
[19] B. Q. Wu and P. L. Leath, Phys. Rev. B **62**, 9338 (2000).
[20] J. M. Hedgepeth and P. Van Dyke, J. Compos. Mater. **1**, 294 (1967).
[21] S. Mahesh, S. L. Phoenix, and I. J. Beyerlein, Int. J. Fract. **115**, 41 (2002).
[22] W. A. Curtin, Phys. Rev. Lett. **80**, 1445 (1998).
[23] W. A. Curtin, Adv. Appl. Mech. **36**, 163 (1999).
[24] W. A. Curtin and H. Scher, Phys. Rev. Lett. **67**, 2457 (1991).

[25] W. A. Curtin and H. Scher, Phys. Rev. B **55**, 12 038 (1997).
[26] W. A. Curtin and H. Scher, Phys. Rev. B **55**, 12 051 (1997).
[27] W. I. Newman and S. L. Phoenix, Phys. Rev. E **63**, 021507 (2001).
[28] W. I. Newman, A. M. Gabirelov, T. A. Durand, S. L. Phoenix, and D. L. Turcotte, Physica D **77**, 200 (1994).
[29] S. L. Phoenix and I. J. Beyerlein, in *Comprehensive Composite Materials*, Vol. 1, edited by A. Kelly and C. Zweben (Elsevier, Amsterdam, 2000).
[30] R. L. Smith, S. L. Phoenix, M. R. Greenfield, R. B. Henstenburg, and R. E. Pitt, Proc. R. Soc. London, Ser. A **388**, 353 (1983).
[31] R. Arratia, L. Goldstein, and L. Gordon, Stat. Sci. **5**, 403 (1990).